

Fermionic partial tomography via classical shadows

Andrew Zhao,^{1,*} Nicholas C. Rubin,^{2,†} and Akimasa Miyake^{1,‡}

¹*Center for Quantum Information and Control, Department of Physics and Astronomy, University of New Mexico, Albuquerque, New Mexico 87106, USA*

²*Google Research, Mountain View, California, 94043, USA*

(Dated: June 3, 2022)

We propose a tomographic protocol for estimating any k -body reduced density matrix (k -RDM) of an n -mode fermionic state, a ubiquitous step in near-term quantum algorithms for simulating many-body physics, chemistry, and materials. Our approach extends the framework of classical shadows, a randomized approach to learning a collection of quantum state properties, to the fermionic setting. Our sampling protocol uses randomized measurement settings generated by a discrete group of fermionic Gaussian unitaries, implementable with linear-depth circuits. We prove that estimating all k -RDM elements to additive precision ε requires on the order of $\binom{n}{k} k^{3/2} \log(n)/\varepsilon^2$ repeated state preparations, which is optimal up to the logarithmic factor. Furthermore, numerical calculations show that our protocol offers a substantial improvement in constant overheads for $k \geq 2$, as compared to prior deterministic strategies. We also adapt our method to particle-number symmetry, wherein the additional circuit depth may be halved at the cost of roughly 2–5 times more repetitions.

Introduction.—One of the most promising applications of quantum computation is the study of strongly correlated systems such as interacting fermions. While quantum algorithms such as phase estimation [1, 2] allow for directly computing important quantities like ground-state energies with quantum speedup [3–5], current hardware limitations [6] have directed much attention toward variational methods. Of note is the variational quantum eigensolver (VQE) [7, 8], where short-depth quantum circuits are repeatedly run and measured in order to estimate observable expectation values. For simulations of many-body quantum systems, the tomographic target is typically the k -body reduced density matrices (k -RDMs).

Initial bounds on the repetition count associated with fermionic two-body Hamiltonians were prohibitively high [9], spurring on much recent work addressing this problem. We roughly classify the strategies into two categories: those which specifically target energy estimates [8, 10–24], referred to as Hamiltonian averaging, and more general techniques which can apply to entire RDMs [25–38]. (Not all works fit neatly into this dichotomy, e.g., Refs. [39–43].) Hamiltonian averaging is ultimately interested in the single observable, allowing for heavy exploitation in its structure. In contrast, reconstructing an RDM requires estimating all the observables which parametrize it.

Though generally more expensive than Hamiltonian averaging, obtaining the k -RDM allows one to determine the average value of any k -body observable [44]. For example, the electronic energy of chemical systems is a linear functional of the 2-RDM, while in condensed-matter systems, effective models for electrons can require knowledge of the 3-RDM [45, 46]. Beyond the energy, other important physical properties include pair-correlation func-

tions and various order parameters [47, 48]. The 2-RDM is also required for a host of error-mitigation techniques in quantum algorithms [13, 49, 50], which have been experimentally demonstrated to be crucial in obtaining accurate results [51–54]. Additionally, promising extensions to VQE such as adaptive ansatz construction [55–58] and multireference- and excited-state calculations [49, 50, 59–62] can require up to $k = 4$.

Motivated by these considerations, in this work we focus on partial tomography for fermionic RDMs. While numerous works have demonstrated essentially optimal sample complexity for estimating qubit RDMs [31, 32, 36–38], such approaches necessarily underperform when naively applied to the fermionic setting. Recognizing this fundamental distinction, Bonet-Monroig *et al.* [32] and Jiang *et al.* [36] provide different strategies which achieve optimal scaling for fermions. Unfortunately, the former construction is not readily generalized for $k > 2$, while the latter requires a doubling in the number of qubits and a particular choice of fermion-to-qubit mapping.

We propose a *randomized* scheme which is free from these obstacles. It is based on the theory of classical shadows [38]: a protocol of randomly distributed measurements from which one acquires a partial classical representation of an unknown quantum state (its “shadow”). Classical shadows are sufficient for learning a limited collection of observables, making this framework ideal for partial state tomography. Our key results are to identify efficient choices for the ensemble of random measurements, suitable for the structure of fermionic observables.

Fermionic RDMs.—Consider a fixed-particle state ρ represented in second quantization on n fermion modes. The k -RDM of ρ , obtained by tracing out all but k particles, is typically written with the matrix elements

$${}^k D_{q_1 \dots q_k}^{p_1 \dots p_k} := \text{tr}(a_{p_1}^\dagger \dots a_{p_k}^\dagger a_{q_k} \dots a_{q_1} \rho), \quad (1)$$

where a_p^\dagger, a_p are fermionic creation and annihilation operators, $p \in \{0, \dots, n-1\}$. By linearity, k -RDM elements

* azhao@unm.edu

† nickrubin@google.com

‡ amiyake@unm.edu

may be equivalently expressed in the Majorana formalism, beginning with the definitions

$$\gamma_{2p} := a_p + a_p^\dagger, \quad \gamma_{2p+1} := -i(a_p - a_p^\dagger). \quad (2)$$

For each $2k$ -combination $\mu \equiv (\mu_1, \dots, \mu_{2k})$, where $0 \leq \mu_1 < \dots < \mu_{2k} \leq 2n-1$, we define a $2k$ -degree Majorana operator

$$\Gamma_\mu := i^k \gamma_{\mu_1} \cdots \gamma_{\mu_{2k}}. \quad (3)$$

All unique $2k$ -degree Majorana operators are indexed by the set of all $2k$ -combinations of $\{0, \dots, 2n-1\}$, which we shall denote by $\mathcal{C}_{2n,2k}$. Since Majorana operators possess the same algebraic properties as Pauli operators (Hermitian, self-inverse, and trace orthogonal), any fermion-to-qubit encoding maps between the two in a one-to-one correspondence.

The commutativity structure inherited onto $\mathcal{C}_{2n,2k}$ constrains the maximum number of mutually commuting (hence simultaneously measurable) operators to be $\mathcal{O}(n^k)$ [32]. As there are $\mathcal{O}(n^{2k})$ independent k -RDM elements, this implies an optimal scaling of $\mathcal{O}(n^k)$ measurement settings to account for all matrix elements.

Classical shadows and randomized measurements.—We briefly review the framework of classical shadows introduced by Huang *et al.* [38], on which we build our fermionic extension and prove sampling bounds. Let ρ be an n -qubit state and $\{O_1, \dots, O_L\}$ a set of L traceless observables for which we wish to learn $\text{tr}(O_1\rho), \dots, \text{tr}(O_L\rho)$. This method employs a simple measurement primitive: for each preparation of ρ , apply the unitary map $\rho \mapsto U\rho U^\dagger$, where U is randomly drawn from some ensemble \mathcal{U} ; then perform a projective measurement in the computational basis, $\{|z\rangle \mid z \in \{0, 1\}^n\}$.

Suppose we have an efficient classical representation for inverting the unitary map on postmeasurement states, yielding $U^\dagger|z\rangle\langle z|U$. Then the process of repeatedly applying the measurement primitive and (classically) inverting the unitary may be viewed, in expectation, as the quantum channel

$$\mathcal{M}_{\mathcal{U}}(\rho) := \mathbb{E}_{U \sim \mathcal{U}, |z\rangle \sim U\rho U^\dagger} [U^\dagger|z\rangle\langle z|U], \quad (4)$$

where $|z\rangle \sim U\rho U^\dagger$ is defined by the usual probability distribution from Born's rule, $\langle z|U\rho U^\dagger|z\rangle$ for all $z \in \{0, 1\}^n$. Informational completeness of \mathcal{U} ensures that this channel is invertible, which allows us to define the classical shadow

$$\hat{\rho}_{U,z} := \mathcal{M}_{\mathcal{U}}^{-1}(U^\dagger|z\rangle\langle z|U) \quad (5)$$

associated with the particular copy of ρ for which U was applied and $|z\rangle$ was obtained. Classical shadows form an unbiased estimator for ρ , and so they can be used to estimate the expectation value of any observable O :

$$\mathbb{E}_{U \sim \mathcal{U}, |z\rangle \sim U\rho U^\dagger} [\text{tr}(O\hat{\rho}_{U,z})] = \text{tr}(O\rho). \quad (6)$$

The number of repetitions M required to obtain an accurate estimate for each $\text{tr}(O_j\rho)$ is controlled by their

estimators' variances, which may be upper bounded by

$$\max_{\text{states } \sigma} \mathbb{E}_{\substack{U \sim \mathcal{U} \\ |z\rangle \sim U\sigma U^\dagger}} [\langle z|U\mathcal{M}_{\mathcal{U}}^{-1}(O_j)U^\dagger|z\rangle^2] =: \|O_j\|_{\mathcal{U}}^2. \quad (7)$$

This quantity is referred to as (the square of) the shadow norm. Then by median-of-means estimation, one may show that

$$M = \mathcal{O}\left(\frac{\log L}{\varepsilon^2} \max_{1 \leq j \leq L} \|O_j\|_{\mathcal{U}}^2\right) \quad (8)$$

suffices to estimate all expectation values to within additive error ε . To optimize Eq. (8) for a fixed collection of observables, the only available freedom is in \mathcal{U} . One must therefore properly choose the ensemble of unitaries with respect to the target observables.

Naive application to fermionic observables.—A natural ensemble to consider for near-term considerations is the group of single-qubit Clifford gates, $\text{Cl}(1)^{\otimes n}$ (i.e., Pauli-basis measurements). For an ℓ -local Pauli observable P , we have $\|P\|_{\text{Cl}(1)^{\otimes n}}^2 = 3^\ell$ [38], similar to the results of a variety of alternative approaches [31, 32, 36, 37]. While optimal for qubit ℓ -RDMs, these measurements cannot achieve the desired $\mathcal{O}(n^k)$ scaling in the fermionic setting due to the inherent nonlocality of fermion-to-qubit mappings. Indeed, assuming that the n fermion modes are encoded into n qubits, the 1-degree Majorana operators necessarily possess an average qubit locality of at least $\log_3(2n)$ [36]. This implies that, under random Pauli-basis measurements, the (squared) shadow norm maximized over all $2k$ -degree Majorana operators cannot do better than $3^{2k \log_3(2n)} = 4^k n^{2k}$. It is then straightforward to check that commonly used mappings, such as the Jordan–Wigner [63] and Bravyi–Kitaev [64–67] transformations, yield even worse scalings (3^n and $\sim 9^k n^{3.2k}$, respectively).

Randomized measurements with fermionic Gaussian unitaries.—In order to obtain optimal scaling in the shadow norm, we propose uniformly randomizing over a different ensemble: the group of fermionic Gaussian Clifford unitaries. First, the group of fermionic Gaussian unitaries $\text{FGU}(n)$ comprises all unitaries of the form

$$U(e^A) := \exp\left(-\frac{1}{4} \sum_{\mu, \nu=0}^{2n-1} A_{\mu\nu} \gamma_\mu \gamma_\nu\right), \quad (9)$$

where $A = -A^\top \in \mathbb{R}^{2n \times 2n}$. Recognizing this condition as the definition of the Lie algebra $\mathfrak{so}(2n)$, we see that $\text{FGU}(n)$ is fully characterized by $\text{SO}(2n)$ [68]. In particular, its adjoint action

$$U(Q)^\dagger \gamma_\mu U(Q) = \sum_{\nu=0}^{2n-1} Q_{\mu\nu} \gamma_\nu \quad \forall Q \in \text{SO}(2n) \quad (10)$$

allows for efficient classical simulation [69–73]. Secondly, the Clifford group $\text{Cl}(n)$ is the set of all unitary transformations which permute n -qubit Pauli operators among

themselves. It also admits an efficient classical representation [74, 75]. Since Majorana operators are equivalent to Pauli operators, we may deduce from Eq. (10) that a unitary which is both Gaussian and Clifford corresponds to Q being a signed permutation matrix. Note that this defines the full group of Majorana swap circuits [32]. As the signs are irrelevant for our purpose, we simply consider the group of $2n \times 2n$ permutation matrices with determinant 1, known as (the faithful matrix representation of) the alternating group, $\text{Alt}(2n)$.

Concretely, we set

$$\mathcal{U}_{\text{FGU}} := \{U(Q) \in \text{FGU}(n) \mid Q \in \text{Alt}(2n)\}. \quad (11)$$

Given the context of fermionic tomography, the motivation for studying $\text{FGU}(n)$ is clear, as it preserves the degree of Majorana operators. On the other hand, the restriction to the discrete Clifford elements turns out to be helpful for practical implementation. As we show in Sec. B of the Supplemental Material (SM), the permutational property necessarily implies that \mathcal{M}_{FGU} , as a linear map on the algebra of fermionic observables, is diagonalized by the Majorana operators,

$$\mathcal{M}_{\text{FGU}}(\Gamma_{\mu}) = \lambda_{\mu} \Gamma_{\mu} \quad \forall \mu \in \mathcal{C}_{2n,2k}, \quad (12)$$

with eigenvalues

$$\lambda_{\mu} = \binom{n}{k} \binom{2n}{2k}^{-1} \equiv \lambda_{n,k}. \quad (13)$$

In this diagonal form, the channel is trivially invertible. Thus we may obtain closed-form expressions for the classical shadows $\hat{\rho}_{Q,z}$, and, importantly, their corresponding estimators for $\text{tr}(\Gamma_{\mu}\rho)$:

$$\text{tr}(\Gamma_{\mu}\hat{\rho}_{Q,z}) = \lambda_{n,k}^{-1} \sum_{\nu \in \mathcal{C}_{2n,2k}} \langle z | \Gamma_{\nu} | z \rangle \det[Q_{\nu,\mu}]. \quad (14)$$

Here, $Q_{\nu,\mu}$ denotes the submatrix of Q formed from its rows and columns indexed by ν and μ , respectively [76]. Since Q is a permutation matrix, for each μ there is exactly one ν' such that $\det[Q_{\nu',\mu}] \neq 0$. Thus Eq. (14) is nonzero if and only if $\Gamma_{\nu'}$ corresponds to a diagonal Majorana operator (i.e., maps to a Pauli- Z operator). In other words, the Clifford operation $U(Q)$ sends Γ_{μ} to $\Gamma_{\nu'}$ (up to a sign), which can be measured only if it is diagonal in the computational basis.

The eigenvalues $\lambda_{n,k}^{-1}$ of the inverse channel turn out to correspond precisely to the shadow norm. The sample complexity of our approach then follows from Eq. (8). We summarize this first key result with the following theorem.

Theorem 1. *Consider all $2k$ -degree Majorana operators Γ_{μ} on n fermionic modes, labeled by $\mu \in \mathcal{C}_{2n,2k}$. Under the ensemble \mathcal{U}_{FGU} defined in Eq. (11), the shadow norm satisfies*

$$\|\Gamma_{\mu}\|_{\text{FGU}}^2 = \binom{2n}{2k} \binom{n}{k}^{-1} \approx \binom{n}{k} \sqrt{\pi k} \quad (15)$$

for all $\mu \in \mathcal{C}_{2n,2k}$. Furthermore, there is no subgroup $G \subset \text{FGU}(n) \cap \text{Cl}(n)$ for which $\|\Gamma_{\mu}\|_G < \|\Gamma_{\mu}\|_{\text{FGU}}$. Thus, the method of classical shadows estimates the fermionic k -RDM of any state ρ , i.e., $\text{tr}(\Gamma_{\mu}\rho)$ for all $\mu \in \bigcup_{j=1}^k \mathcal{C}_{2n,2j}$, to additive error ε , given

$$M = \mathcal{O}\left[\binom{n}{k} \frac{k^{3/2} \log n}{\varepsilon^2}\right] \quad (16)$$

copies of ρ .

The proof is presented in the SM, Sec. B. Note that, because $-\lambda_{n,k}^{-1} \leq \text{tr}(\Gamma_{\mu}\hat{\rho}_{Q,z}) \leq \lambda_{n,k}^{-1}$ [from Eq. (14)], Hoeffding's inequality [77] guarantees the above sample complexity with a standard sample-mean estimator, rather than requiring the median-of-means technique proposed in the original work [38].

This result has an intuitive conceptual interpretation. In the computational basis, there are precisely $\binom{n}{k}$ diagonal Majorana operators within $\mathcal{C}_{2n,2k}$, corresponding to the unique k -fold products of occupation-number operators on n modes. As a permutation on $\mathcal{C}_{2n,2k}$, each element of \mathcal{U}_{FGU} defines a different basis in which some other subset of $\binom{n}{k}$ operators are diagonal. Then, one may expect to account for all $|\mathcal{C}_{2n,2k}| = \binom{2n}{2k}$ Majorana operators by randomly selecting on the order of $\binom{2n}{2k}/\binom{n}{k}$ such bases; Theorem 1 makes this claim rigorous.

Fermionic Gaussian unitaries have a well-studied compilation scheme based on a Givens rotation decomposition [78–80]. When the unitary has neither particle-number nor spin symmetry, as is the case for a general element of \mathcal{U}_{FGU} , we require a circuit depth of at most $2n-1$ with respect to this decomposition [80]. Additionally, as pointed out in Ref. [32], Gaussian unitaries commute with the global parity operator $\Gamma_{(0,\dots,2n-1)}$, allowing for error mitigation via symmetry verification [81, 82].

Such compilation schemes make use of a group homomorphism property, $U(Q_1)U(Q_2) = U(Q_1Q_2)$. Therefore, if the circuit preparing ρ itself features any such operations at the end, then we may further compile the measurement unitary into the state-preparation circuit [50]. In the case of indefinite particle number, this concatenation is essentially free. However, for systems with particle-number symmetry, these rotations have depth at most n [79, 80], so they must be embedded into the larger, general Gaussian unitary. This observation motivates us to explore the classical shadows approach over the number-conserving (NC) subgroup of $\text{FGU}(n)$.

Modification based on particle-number symmetry.— Gaussian unitaries which preserve particle number are more naturally parametrized by $\text{U}(n)$ rather than $\text{SO}(2n)$. That is, we write

$$U(e^{\kappa}) := \exp\left(\sum_{p,q=0}^{n-1} \kappa_{pq} a_p^{\dagger} a_q\right), \quad (17)$$

where $\kappa = -\kappa^{\dagger} \in \mathbb{C}^{n \times n}$. The $\text{U}(1)$ particle-number symmetry manifests as a global phase factor of $e^{\text{tr} \kappa/2}$, so

without loss of generality we may take $\kappa \in \mathfrak{su}(n)$. Such unitaries are also called orbital basis rotations, owing to their adjoint action,

$$U(u)^\dagger a_p U(u) = \sum_{q=0}^{n-1} u_{pq} a_q \quad \forall u \in \mathrm{SU}(n). \quad (18)$$

This action on Majorana operators may be computed by linear extension.

Taking the intersection with the Clifford group requires that u be an $n \times n$ generalized permutation matrix, with nonzero elements taking values in $\{\pm 1, \pm i\}$. This corresponds to the full group of fermionic swap circuits [64, 79]. Again, the phase factors in u are irrelevant, so we restrict to $u \in \mathrm{Alt}(n)$. By itself, this ensemble is insufficient to perform tomography. To see this, consider an arbitrary k -RDM operator $A_{\mathbf{p}}^\dagger A_{\mathbf{q}} := a_{p_1}^\dagger \cdots a_{p_k}^\dagger a_{q_k} \cdots a_{q_1}$, where $\mathbf{p}, \mathbf{q} \in \mathcal{C}_{n,k}$. Such operators have nonzero diagonal matrix elements in the computational basis if and only if $\mathbf{p} = \mathbf{q}$. Informational completeness thus requires that there exists some $U(u)$ which maps $A_{\mathbf{p}}^\dagger A_{\mathbf{q}}$ to $A_{\mathbf{p}'}^\dagger A_{\mathbf{p}'}$ for some $\mathbf{p}' \in \mathcal{C}_{n,k}$. However, since $u \in \mathrm{Alt}(n)$, conjugation by $U(u)$ simply permutes each \mathbf{p} and \mathbf{q} separately. Due to bijectivity, there is no permutation which sends both \mathbf{p} and \mathbf{q} to the same \mathbf{p}' if $\mathbf{p} \neq \mathbf{q}$.

The ensemble thus necessarily requires operations beyond either the NC or Gaussian constraints. The simplest option for maintaining the low-depth structure of the fermionic basis rotations is to perform Pauli measurements at the end of the circuit, which are already known to be informationally complete. Although the resulting circuit does not preserve particle number, this addition only incurs a single layer of single-qubit gates. Formally, we define the ensemble

$$\mathcal{U}_{\mathrm{NC}} := \{V \circ U(u) \mid V \in \mathrm{Cl}(1)^{\otimes n}, u \in \mathrm{Alt}(n)\}. \quad (19)$$

By virtue of introducing the notion of “single-qubit” gates, this method is dependent on the choice of fermion-to-qubit mapping. Let $\mathrm{loc}(\Gamma_\mu)$ denote the qubit locality of Γ_μ under some chosen mapping. While the Pauli measurements incur the usual factor of $3^{\mathrm{loc}(\cdot)}$ in the shadow norm, the variance is substantially reduced through the randomization over fermionic swap circuits, which effectively averages over the qubit localities of all Majorana operators of the same degree (rather than scaling with the worst-case locality). Specifically, we find that the shadow norm takes the form

$$\|\Gamma_\mu\|_{\mathrm{NC}}^2 = \mathbb{E}_{u \sim \mathrm{Alt}(n)} \left[3^{-\mathrm{loc}[U(u)^\dagger \Gamma_\mu U(u)]} \right]^{-1}. \quad (20)$$

Although this expression is unlikely to possess a closed form, the following theorem gives a universal bound on its tomographic efficiency.

Theorem 2. *Under the ensemble $\mathcal{U}_{\mathrm{NC}}$ defined in Eq. (19), the shadow norm obeys*

$$\max_{\mu \in \mathcal{C}_{2n,2k}} \|\Gamma_\mu\|_{\mathrm{NC}}^2 \leq 9^k \binom{n}{2k} \binom{n-k}{k}^{-1} = \mathcal{O}(n^k) \quad (21)$$

for a fixed integer k and for all fermion-to-qubit mappings. Thus the method of classical shadows estimates the k -RDM to additive error ε with sample complexity

$$M = \mathcal{O}\left(\frac{n^k \log n}{\varepsilon^2}\right). \quad (22)$$

We provide derivations for the above results in the SM, Sec. C. Note that we have fixed k as a constant here, and so the asymptotic notation may hide potentially large prefactors depending on k . To understand these practical performance details, we turn to numerical studies.

Numerical calculations.—Instead of drawing a new circuit for each repetition, here we employ a simplification more amenable to practical implementation. Fixing some integer $r \geq 1$, we generate a random collection $\{U^{(j)} \sim \mathcal{U}\}_{j=1}^{K_r}$ of K_r unitaries such that all target observables are covered at least r times. That is, given $U(Q) \in \mathcal{U}_{\mathrm{FGU}}$, the covered $2k$ -degree operators Γ_μ correspond to those for which $\det[Q_{\nu,\mu}] \neq 0$, where each Γ_ν is diagonal [recall Eq. (14) and the surrounding discussion]. For the $\mathcal{U}_{\mathrm{NC}}$ calculations, the qubit encodings were automated through OpenFermion [83].

To achieve accuracy corresponding to $S = \mathcal{O}(1/\varepsilon^2)$ samples per observable, one then repeats each measurement circuit $[S/r]$ times. For simplicity, let $S/r \in \mathbb{N}$; the total number of circuit repetitions for our randomized protocols is then SK_r/r . To compare this value against that of prior strategies, all of which are deterministic, the number of repetitions is calculated as $S \times C$, where C is the number of sets of mutually commuting observables constructed by those methods.

Although K_r naturally grows with r , this relation is typically sublinear, since the random measurement bases become more uniformly and efficiently allocated as more of them are drawn. Thus K_r/r tends to decrease as a function of r (for a demonstration of this effect, see Sec. E 1 in the SM). As it is not practical to use arbitrarily large values of r due to the classical preprocessing resources, we have fixed $r = 50$.

For our comparisons presented in Fig. 1, we focus on the most competitive prior strategies applicable to fermionic RDM tomography. Since the 1-RDM has a relatively simple structure, optimal strategies are known [32, 54], and so we find that randomization underperforms for $k = 1$. However, the advantage of our $\mathcal{U}_{\mathrm{FGU}}$ -based method becomes clear for $k \geq 2$. While SORTED INSERTION [17] (a tractable stand-in for the memory-intensive algorithms based on approximately solving NP-hard graph problems [28–30, 34]) has a slight advantage for very small n , its unfavorable scaling is quickly apparent. On the other hand, comparing against the Majorana clique cover which does feature optimal scaling [32], we observe a consistent, roughly twofold factor, improvement with our method for $k = 2$.

For the $\mathcal{U}_{\mathrm{NC}}$ case, we see a trade-off between circuit depth and measurement efficiency. First, we observe the expected dependence on the choice of fermion-to-qubit

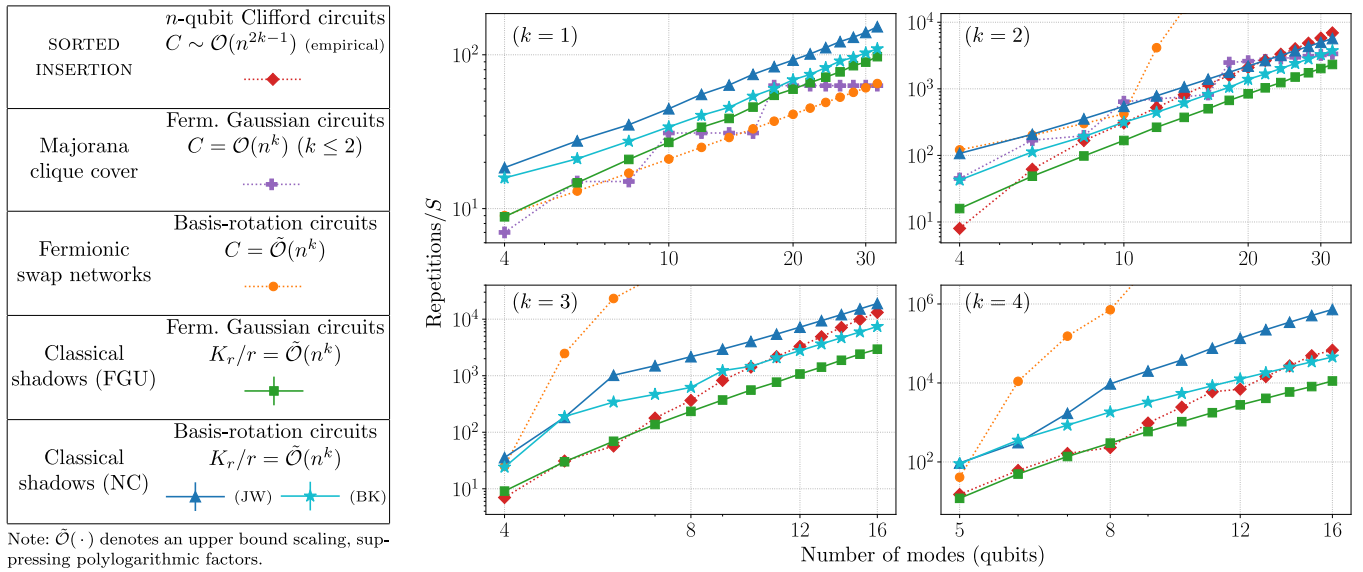


FIG. 1. (Left): Summary of the methods compared here, cataloging their required circuit types and scalings in the number of measurement settings. Since graph-based methods [28–30, 34] are resource-intensive, we employ SORTED INSERTION [17] as a tractable alternative which retains the notion of general qubit commutativity. The Majorana clique cover [32], which employs the same class of Gaussian Clifford circuits as our classical shadows (FGU) unitaries, possesses optimal asymptotic scaling, but it exhibits jumps at powers of 2 due to a divide-and-conquer approach. The measurement strategy using fermionic swap networks is a generalization of the optimal 1-RDM strategy introduced Ref. [54], which we describe in Sec. D of the SM. (Right): Numerical performance of the methods for estimating fermionic k -RDMs (log-log scale). Note that SORTED INSERTION and the Majorana clique cover are equivalent for $k = 1$. Since our scheme uses randomization, we include bars of 1 standard deviation, averaged over 10 instances. Note however that they are too small compared to the scale of the plots to be seen, indicating the consistency of our method.

mapping, with the Jordan–Wigner (JW) mapping performing worse due to higher qubit locality. While more circuits are required compared to the \mathcal{U}_{FGU} case (e.g., a factor of $\sim 2\text{--}5$ under the Bravyi–Kitaev (BK) mapping, depending on k), each circuit itself requires only half the depth of general Gaussian measurements (i.e., of both our \mathcal{U}_{FGU} -based method and the Majorana clique cover [32]). Notably, however, NC classical shadows for the 2-RDM under the Bravyi–Kitaev mapping is closely comparable to the Majorana clique cover.

Conclusions.—We have adapted the framework of classical shadows to the efficient tomography of fermionic k -RDMs, applicable for all k . Numerical calculations demonstrate that our approach consistently outperforms prior deterministic strategies using quantum circuits of comparable sizes when $k \geq 2$, despite the logarithmic factor in the sample complexity resulting from rigorous bounds for worst-case probabilistic instances. The power of randomization here lies in avoiding the NP-hard problem of partitioning observables into mutually commuting cliques [27–30]. Our results indicate that a highly re-

dundant covering of the target observables, with much overlap between the randomly drawn cliques, suffices to efficiently perform the actual task of *tomography*, since a factor of $\mathcal{O}(1/\varepsilon^2)$ repetitions is already required to estimate each observable accurately.

An outlook for further applications is to adapt these ensembles, e.g., for Hamiltonian averaging. Our method is expectedly less efficient in this context than those tailored for estimating a single observable (see Sec. E 3 in the SM for preliminary numerical calculations). Possible modifications may include biasing the distribution of unitaries [23], or derandomization techniques [38, 84, 85].

We thank Hsin-Yuan (Robert) Huang and Charles Hadfield for helpful discussions. This work was supported partially by the National Science Foundation STAQ project (PHY 1818914), QLCI Q-SEnSE award (OMA 2016244), CHE 2037832, and the Department of Energy Center Quantum Systems Accelerator. We acknowledge the use of high-performance computing resources provided by the UNM Center for Advanced Research Computing, supported in part by the National Science Foundation.

Supplemental Material

CONTENTS

| | |
|---|----|
| A. Additional notation | 6 |
| B. Computations with the fermionic Gaussian Clifford ensemble | 7 |
| 1. The classical shadows channel | 7 |
| 2. The shadow norm | 10 |
| 3. The classical shadow estimator | 15 |
| 4. Expressions for arbitrary observables | 15 |
| 5. Performance guarantees without median-of-means estimation | 17 |
| C. Computations with the number-conserving modification | 18 |
| 1. The shadow norm | 18 |
| 2. Universal upper bounds on the shadow norm | 19 |
| D. Fermionic swap network bounds | 21 |
| 1. The 1-RDM method | 21 |
| 2. The 2-RDM method | 22 |
| 3. A k -RDM generalization | 23 |
| a. Upper bounds for $k = 3, 4$ | 23 |
| E. Supplementary numerical calculations | 25 |
| 1. Hyperparameter tuning | 25 |
| 2. Realistic time estimates | 25 |
| 3. Hamiltonian averaging | 26 |
| References | 28 |

Appendix A: Additional notation

First, we define some notation and preliminary concepts not discussed in the main text. For completeness, we generalize the definition of Majorana operators to include odd-degrees:

$$\Gamma_{\boldsymbol{\mu}} := i^{(k)} \gamma_{\mu_1} \cdots \gamma_{\mu_k}, \quad (\text{A1})$$

where $\boldsymbol{\mu} \in \mathcal{C}_{2n,k}$. Where required, we may define the empty product ($k = 0$) as the identity, i.e., $\Gamma_{\emptyset} := \mathbb{1}$. Then for each $0 \leq k \leq 2n$, we define the \mathbb{R} -linear span of k -degree Majorana operators on n modes,

$$\mathcal{A}_k^{(n)} := \text{span}\{\Gamma_{\boldsymbol{\mu}} \mid \boldsymbol{\mu} \in \mathcal{C}_{2n,k}\}, \quad (\text{A2})$$

which is isomorphic (as a vector space) to $\mathbb{R}^{\binom{2n}{k}}$. The algebra of even-degree fermionic observables shall be denoted by

$$\mathcal{A}_{\text{even}}^{(n)} := \bigoplus_{k=0}^n \mathcal{A}_{2k}^{(n)}. \quad (\text{A3})$$

Due to the parity superselection rule [86], physical fermionic operators lie in $\mathcal{A}_{\text{even}}^{(n)}$; thus the notions of informational completeness for tomography are understood with respect to this constraint. To see this, suppose we interpret $|z\rangle$ as a Fock basis state. Only products of occupation-number operators, $\prod_p a_p^\dagger a_p$ (modulo anticommutation relations), have nonzero diagonal elements in the Fock basis. Thus if U is a unitary generated by a fermionic Hamiltonian (hence also respecting the parity supersymmetry), only those $O \in \mathcal{A}_{\text{even}}^{(n)}$ are able to satisfy $\langle z|OUU^\dagger|z\rangle \neq 0$. This argument also holds if one insists on viewing $|z\rangle$ as a qubit computational basis state, since they necessarily map to Fock basis states [87].

The group of fermionic Gaussian unitaries $\text{FGU}(n)$ is generated by $i\mathcal{A}_2^{(n)}$, and its adjoint action on any k -degree Majorana operator straightforwardly generalizes as

$$U(Q)^\dagger \Gamma_\mu U(Q) = \sum_{\nu \in \mathcal{C}_{2n,k}} \det[Q_{\mu,\nu}] \Gamma_\nu, \quad (\text{A4})$$

where $Q_{\mu,\nu}$ denotes the submatrix formed by taking the rows and columns of Q indexed by μ and ν , respectively [76, Appendix A]. This defines an adjoint representation $\text{FGU}(n) \rightarrow \text{SO}[\mathfrak{su}(2^n)] \cong \text{SO}(4^n - 1)$, understood in the sense that $\text{FGU}(n) \subseteq \text{SU}(2^n)$. We will rather be interested in the orthogonal representation of $\text{SO}(2n)$ induced by the adjoint representation through the group homomorphism $U: \text{SO}(2n) \rightarrow \text{FGU}(n)$. That is, we define $\Phi: \text{SO}(2n) \rightarrow \text{SO}(4^n - 1)$ by the matrix elements

$$[\Phi(Q)]_{\mu\nu} := \det[Q_{\mu,\nu}]. \quad (\text{A5})$$

By the Cauchy–Binet formula one may verify that this indeed defines an orthogonal matrix. Additionally, Φ inherits the homomorphism property from U ; hence it is an orthogonal representation.

Since determinants are defined only for square matrices, Φ possesses a natural decomposition as $\Phi = \bigoplus_{k=1}^{2n} \phi_k$, where each $\phi_k: \text{SO}(2n) \rightarrow \text{SO}(\mathcal{A}_k^{(n)}) \cong \text{SO}[\binom{2n}{k}]$ is defined just as in Eq. (A5), restricted a particular k . These subrepresentations will be the main focus of our analysis.

Finally, because of their relation to the Clifford group, we make frequent use of permutations and their generalizations. We establish the relevant notation here. Let $d, m > 0$ be integers. We denote the symmetric group on d symbols by $\text{Sym}(d)$, which is faithfully represented by the group of $d \times d$ permutation matrices. The alternating group $\text{Alt}(d)$ is the subgroup of all even parity permutations. The generalized symmetric group of cyclic order m over d symbols is defined via the wreath product, $\text{Sym}(m, d) := \mathbb{Z}_m \wr \text{Sym}(d) \cong \mathbb{Z}_m^d \rtimes \text{Sym}(d)$. Its faithful matrix representation is the group of $d \times d$ generalized permutation matrices, wherein each nonzero matrix element can take on values from the m th roots of unity. The determinant of such matrices is the sign of the underlying permutation, multiplied by all d nonzero elements. In particular, we shall refer to $\text{Sym}(2, d)$ as the group of signed permutation matrices, and denote its $+1$ determinant subgroup by $\text{Sym}^+(2, d)$.

Appendix B: Computations with the fermionic Gaussian Clifford ensemble

We now derive the main results leading to Theorem 1 of the main text. In Appendix B 1 we find an expression for the channel \mathcal{M}_{FGU} , showing that the permutational property of the Clifford group necessarily implies that the channel is diagonalized by the basis of Majorana operators [Eq. (B11)]. Then in Appendix B 2 we compute the corresponding eigenvalues of \mathcal{M}_{FGU} , which are directly related to the ensemble’s shadow norm (Lemma 6). In particular, Lemma 6 provides necessary and sufficient conditions for saturating the minimum value of the shadow norm under Gaussian Clifford measurements. In Theorem 11 we explicitly calculate this minimum value, and finally with Theorem 13 we prove that both $\text{FGU}(n) \cap \text{Cl}(n)$ and its $\text{Alt}(2n)$ -generated subgroup \mathcal{U}_{FGU} (the one presented in the main text) satisfy the necessary and sufficient conditions.

After proving these main results, in Appendix B 3 we explicitly derive the expression for the classical shadows $\hat{\rho}_{Q,z}$. For completeness, we show how to compute the shadow norm for an arbitrary observable in Appendix B 4. Finally, in Appendix B 5 we show how the boundedness of our classical shadow estimators and Hoeffding’s inequality allow us to avoid requiring median-of-means estimation, as discussed in the main text.

1. The classical shadows channel

Our goal is to find an analytic expression for the channel $\mathcal{M}_{\text{FGU}}: \mathcal{A}_{\text{even}}^{(n)} \rightarrow \mathcal{A}_{\text{even}}^{(n)}$,

$$\begin{aligned} \mathcal{M}_{\text{FGU}}(O) &= \mathbb{E}_{U \sim \text{FGU}(n) \cap \text{Cl}(n)} \left[\sum_{z \in \{0,1\}^n} \langle z | U O U^\dagger | z \rangle U^\dagger | z \rangle \langle z | U \right] \\ &= \mathbb{E}_{Q \sim \text{Sym}^+(2, 2n)} \left[\sum_{z \in \{0,1\}^n} \langle z | U(Q) O U(Q)^\dagger | z \rangle U(Q)^\dagger | z \rangle \langle z | U(Q) \right]. \end{aligned} \quad (\text{B1})$$

Since this is a linear map, we need only to evaluate it on a basis of $\mathcal{A}_{\text{even}}^{(n)}$, the most natural choice being the Majorana operators. Distinguishing the Majorana operators which are diagonal (with respect to the computational basis) is

highly important. For each $1 \leq k \leq n$, we shall define the subset $\mathcal{D}_{2n,2k} \subseteq \mathcal{C}_{2n,2k}$ of $2k$ -combinations corresponding to the diagonal $2k$ -degree Majorana operators. Formally,

$$\mathcal{D}_{2n,2k} := \{\boldsymbol{\mu} \in \mathcal{C}_{2n,2k} \mid \langle z | \Gamma_{\boldsymbol{\mu}} | z \rangle \neq 0 \ \forall z \in \{0,1\}^n\}. \quad (\text{B2})$$

Since there are $\binom{n}{k}$ independent k -fold products of occupation-number operators, each set has cardinality $|\mathcal{D}_{2n,2k}| = \binom{n}{k}$, so that

$$\left| \bigcup_{k=1}^n \mathcal{D}_{2n,2k} \right| = \sum_{k=1}^n \binom{n}{k} = 2^n - 1, \quad (\text{B3})$$

which indeed matches the maximal number of simultaneously commuting Pauli operators [88] (e.g., all Pauli- Z operators). For instance, under the Jordan–Wigner transformation, the diagonal operators correspond to the sets

$$\begin{aligned} \mathcal{D}_{2n,2} &:= \{(p, p+1) \mid 0 \leq p \leq 2n-2 : p \text{ even}\}, \\ \mathcal{D}_{2n,4} &:= \{(p, p+1, q, q+1) \mid 0 \leq p < q \leq 2n-2 : p, q \text{ even}\}, \\ \mathcal{D}_{2n,6} &:= \{(p, p+1, q, q+1, r, r+1) \mid 0 \leq p < q < r \leq 2n-2 : p, q, r \text{ even}\}, \end{aligned} \quad (\text{B4})$$

and so forth up to $\mathcal{D}_{2n,2n}$.

With this formalism, we can express the basis states as

$$|z\rangle\langle z| = \frac{1}{2^n} \left(\mathbb{1} + \sum_{j=1}^n \sum_{\boldsymbol{\mu} \in \mathcal{D}_{2n,2j}} \langle z | \Gamma_{\boldsymbol{\mu}} | z \rangle \Gamma_{\boldsymbol{\mu}} \right), \quad (\text{B5})$$

which undergo fermionic Gaussian evolution as

$$\begin{aligned} U(Q)^\dagger |z\rangle\langle z| U(Q) &= \frac{1}{2^n} \left(\mathbb{1} + \sum_{j=1}^n \sum_{\boldsymbol{\mu} \in \mathcal{D}_{2n,2j}} \langle z | \Gamma_{\boldsymbol{\mu}} | z \rangle U(Q)^\dagger \Gamma_{\boldsymbol{\mu}} U(Q) \right) \\ &= \frac{1}{2^n} \left(\mathbb{1} + \sum_{j=1}^n \sum_{\boldsymbol{\mu} \in \mathcal{D}_{2n,2j}} \langle z | \Gamma_{\boldsymbol{\mu}} | z \rangle \sum_{\boldsymbol{\nu} \in \mathcal{C}_{2n,2j}} \det[Q_{\boldsymbol{\mu},\boldsymbol{\nu}}] \Gamma_{\boldsymbol{\nu}} \right). \end{aligned} \quad (\text{B6})$$

For the corresponding probability factor, we use the fact that, since U is a group homomorphism, inverses are preserved [$U(Q)^\dagger = U(Q^\top)$], and so for any $\boldsymbol{\tau} \in \mathcal{C}_{2n,2k}$ we have

$$\begin{aligned} \langle z | U(Q) \Gamma_{\boldsymbol{\tau}} U(Q)^\dagger | z \rangle &= \sum_{\boldsymbol{\sigma} \in \mathcal{C}_{2n,2k}} \det[(Q^\top)_{\boldsymbol{\tau},\boldsymbol{\sigma}}] \langle z | \Gamma_{\boldsymbol{\sigma}} | z \rangle \\ &= \sum_{\boldsymbol{\sigma} \in \mathcal{D}_{2n,2k}} \det[(Q^\top)_{\boldsymbol{\tau},\boldsymbol{\sigma}}] \langle z | \Gamma_{\boldsymbol{\sigma}} | z \rangle. \end{aligned} \quad (\text{B7})$$

Recall some basic properties of Majorana (equiv. Pauli) operators. They are traceless,

$$\sum_{z \in \{0,1\}^n} \langle z | \Gamma_{\boldsymbol{\sigma}} | z \rangle = \text{tr} \Gamma_{\boldsymbol{\sigma}} = 0, \quad (\text{B8})$$

and more generally they are trace orthogonal,

$$\text{tr}(\Gamma_{\boldsymbol{\sigma}} \Gamma_{\boldsymbol{\mu}}) = 2^n \delta_{\boldsymbol{\sigma},\boldsymbol{\mu}}. \quad (\text{B9})$$

In the case that $\Gamma_{\boldsymbol{\sigma}}$ and $\Gamma_{\boldsymbol{\mu}}$ are both diagonal, we have that

$$\begin{aligned} \sum_{z \in \{0,1\}^n} \langle z | \Gamma_{\boldsymbol{\sigma}} | z \rangle \langle z | \Gamma_{\boldsymbol{\mu}} | z \rangle &= \sum_{z \in \{0,1\}^n} \langle z | \Gamma_{\boldsymbol{\sigma}} \Gamma_{\boldsymbol{\mu}} | z \rangle \\ &= \text{tr}(\Gamma_{\boldsymbol{\sigma}} \Gamma_{\boldsymbol{\mu}}) = 2^n \delta_{\boldsymbol{\sigma},\boldsymbol{\mu}}. \end{aligned} \quad (\text{B10})$$

With these relations in hand, we multiply Eqs. (B6) and (B7) and sum over $z \in \{0, 1\}^n$ to obtain

$$\begin{aligned} \sum_{z \in \{0, 1\}^n} \langle z | U(Q) \Gamma_{\tau} U(Q)^\dagger | z \rangle U(Q)^\dagger | z \rangle \langle z | U(Q) &= \frac{1}{2^n} \sum_{\sigma \in \mathcal{D}_{2n,2k}} \det[(Q^\top)_{\tau,\sigma}] \left(\text{tr}(\Gamma_{\sigma}) \mathbb{1} \right. \\ &\quad \left. + \sum_{j=1}^n \sum_{\mu \in \mathcal{D}_{2n,2j}} 2^n \delta_{\sigma\mu} \sum_{\nu \in \mathcal{C}_{2n,2j}} \det[Q_{\mu,\nu}] \Gamma_{\nu} \right) \\ &= \sum_{\substack{\sigma \in \mathcal{D}_{2n,2k} \\ \nu \in \mathcal{C}_{2n,2k}}} \det[Q_{\sigma,\tau}] \det[Q_{\sigma,\nu}] \Gamma_{\nu}. \end{aligned} \quad (\text{B11})$$

One may be tempted to use the Cauchy–Binet formula to evaluate the sum over σ ; crucially, however, the sum is restricted to $\mathcal{D}_{2n,2k}$, so the identity does not apply here. Instead, we will first evaluate the sum over ν by formalizing our notion of Gaussian Clifford transformations as degree-preserving permutations of Majorana operators. For generality, we state the following lemma with regards to any generalized permutation matrix.

Lemma 3. *Let $Q \in \text{Sym}(m, d)$ and fix $\tau \in \mathcal{C}_{d,j}$, $1 \leq j \leq d$. Then there exists exactly one $\sigma \in \mathcal{C}_{d,j}$ for which $|\det[Q_{\sigma,\tau}]| = 1$; otherwise, $\det[Q_{\sigma,\tau}] = 0$. In particular, we have*

$$\det[(Q^\dagger)_{\tau,\sigma}] \det[Q_{\sigma,\nu}] = |\det[Q_{\sigma,\tau}]| \delta_{\tau\nu} \quad (\text{B12})$$

for all $\nu \in \mathcal{C}_{d,j}$.

Proof. By definition of (generalized) permutation matrices, for each column q of Q there is exactly one row p for which $Q_{pq} \neq 0$. Furthermore, this row is unique to each column. This property generalizes from matrix elements to subdeterminants: for each set of columns indexed by τ , there is exactly one unique set of rows σ for which $Q_{\sigma,\tau}$ has a nonzero element in each row. In other words, $Q_{\sigma,\tau} \in \text{Sym}(m, j)$ and hence $|\det[Q_{\sigma,\tau}]| = 1$ (recall that the determinant of these matrices is the sign of the underlying permutation multiplied by m th roots of unity). Otherwise, for all $\sigma' \neq \sigma$, $Q_{\sigma',\tau}$ possesses at least one row or column of all zeros, and hence has determinant 0.

Next, we show that submatrices behave under conjugate transposition as $(Q_{\sigma,\tau})^\dagger = (Q^\dagger)_{\tau,\sigma}$, which can be seen by examining their matrix elements:

$$[Q_{\sigma,\tau}]_{pq} = Q_{\sigma_p \tau_q} = [Q^\dagger]_{\tau_q \sigma_p}^* = [(Q^\dagger)_{\tau,\sigma}]_{qp}^* = [((Q^\dagger)_{\tau,\sigma})^\dagger]_{pq}. \quad (\text{B13})$$

Since the determinant is invariant under transposition and preserves complex conjugation, $\det[(Q^\dagger)_{\tau,\sigma}] = \det[(Q_{\sigma,\tau})]^*$. This gives us

$$\det[(Q^\dagger)_{\tau,\sigma}] \det[Q_{\sigma,\nu}] = \det[(Q_{\sigma,\tau})]^* \det[Q_{\sigma,\nu}]. \quad (\text{B14})$$

But since τ is the unique j -combination for which $\det[(Q_{\sigma,\tau})] \neq 0$ for a fixed σ , the above expression can only be nonzero when $\nu = \tau$. Equation (B12) thus follows. \square

Remark 4. *This uniqueness property of nonzero subdeterminants implies that the image of the orthogonal representation $\Phi: \text{SO}(2n) \rightarrow \text{SO}(4^n - 1)$, when restricted to a subgroup $G \subseteq \text{Sym}^+(2, 2n) \subset \text{SO}(2n)$, lies in $\text{Sym}^+(2, 4^n - 1)$. Its subrepresentations also satisfy $\phi_k(G) \subseteq \text{Sym}[2, \binom{2n}{k}]$. From a physical perspective, these are all straightforward consequences of the Clifford property imposed on our unitary ensemble.*

Applying Lemma 3 to Eq. (B11) reveals that the Majorana operators are in fact the eigenbasis of \mathcal{M}_{FGU} :

$$\begin{aligned} \mathcal{M}_{\text{FGU}}(\Gamma_{\tau}) &= \mathbb{E}_{Q \sim \text{Sym}^+(2, 2n)} \left[\sum_{z \in \{0, 1\}^n} \langle z | U(Q) \Gamma_{\tau} U(Q)^\dagger | z \rangle U(Q)^\dagger | z \rangle \langle z | U(Q) \right] \\ &= \mathbb{E}_{Q \sim \text{Sym}^+(2, 2n)} \left[\sum_{\sigma \in \mathcal{D}_{2n,2k}} |\det[Q_{\sigma,\tau}]| \right] \Gamma_{\tau}. \end{aligned} \quad (\text{B15})$$

2. The shadow norm

To evaluate the eigenvalues of Eq. (B15), we invoke the theory of finite frames [89, 90]. We begin with the definition of a frame.

Definition 5. Let V be a Hilbert space with inner product $\langle \cdot, \cdot \rangle$. A frame is a sequence $\{x_j\}_j \subset V$ which satisfies

$$\alpha \|v\|_V^2 \leq \sum_j |\langle x_j, v \rangle|^2 \leq \beta \|v\|_V^2 \quad \forall v \in V, \quad (\text{B16})$$

for some real constants $\alpha, \beta > 0$ (called the frame bounds). Here, $\|v\|_V := \sqrt{\langle v, v \rangle}$. A frame is called tight if $\alpha = \beta$.

Recall that $\det[Q_{\sigma, \tau}]$ defines the matrix elements of the orthogonal representation $\phi_{2k}: \text{SO}(2n) \rightarrow \text{SO}[\binom{2n}{2k}]$. In order to demonstrate the optimality of our ensemble, we shall generalize Eq. (B15) to take the average over any subgroup $G \subseteq \text{Sym}^+(2, 2n)$, in which case we consider the restricted representations $\phi_{2k}|_G: G \rightarrow \text{SO}[\binom{2n}{2k}]$. (Whenever the context is clear, we shall simply write ϕ_{2k} .) To simplify notation, we take $\mathbb{R}^{\binom{2n}{2k}}$ as our representation space, spanned by the standard basis $\{e_{\mu} \mid \mu \in \mathcal{C}_{2n, 2k}\}$.

Consider the group orbit

$$\phi_{2k}(G)e_{\sigma} := \{\phi_{2k}(Q)e_{\sigma} \mid Q \in G\}. \quad (\text{B17})$$

A sufficient condition for the eigenvalues of \mathcal{M}_G to be nonzero (hence guaranteeing the existence of \mathcal{M}_G^{-1}) is that $\phi_{2k}(G)e_{\sigma}$ be a frame for some $\sigma \in \mathcal{D}_{2n, 2k}$. Indeed, assuming the frame condition, we have

$$\begin{aligned} \mathbb{E}_{Q \sim G} |\det[Q_{\sigma, \tau}]| &= \frac{1}{|G|} \sum_{Q \in G} |\det[Q_{\sigma, \tau}]|^2 \\ &= \frac{1}{|G|} \sum_{Q \in G} |\langle \phi_{2k}(Q)^T e_{\sigma}, e_{\tau} \rangle|_2^2 \\ &\geq \frac{\alpha}{|G|} \|e_{\tau}\|_2^2 > 0 \end{aligned} \quad (\text{B18})$$

for all $\tau \in \mathcal{C}_{2n, 2k}$. Note that the transpose is irrelevant since G is a group. While \mathcal{M}_G may be made positive even without taking G to be a group, the group structure has desirable implications for the measurement complexity (shadow norm) of our scheme. (It is also generally easier to sample from a well-established group like the symmetric group, rather than some ad hoc subset of $\text{Sym}^+(2, 2n)$.) To see this, we shall focus attention exclusively to tight frames, which is motivated by the following observation.

Lemma 6. Let $G \subseteq \text{Sym}^+(2, 2n)$ be a subset such that $\phi_{2k}(G)e_{\sigma}$ is a frame for all $\sigma \in \mathcal{D}_{2n, 2k}$, $1 \leq k \leq n$. Let $\alpha_k, \beta_k > 0$ be the cumulative frame bounds over all σ for each k , i.e.,

$$\alpha_k \leq \frac{1}{|G|} \sum_{\sigma \in \mathcal{D}_{2n, 2k}} \sum_{Q \in G} |\det[Q_{\sigma, \tau}]|^2 \leq \beta_k \quad (\text{B19})$$

for all $\tau \in \mathcal{C}_{2n, 2k}$. Then the shadow norm associated with the ensemble G satisfies

$$\alpha_k / \beta_k^2 \leq \|\Gamma_{\tau}\|_G^2 \leq \beta_k / \alpha_k^2. \quad (\text{B20})$$

These bounds are saturated if and only if the cumulative frame is tight, i.e., $\|\Gamma_{\tau}\|_G^2 = \alpha_k^{-1}$.

Remark 7. In Eq. (B19), and hence in Eq. (B15), the actual frame being used is $\phi_{2k}(G)(e_{\sigma}|G|^{-1/2})$, i.e., the “orbit” of the basis vector scaled by a factor of $|G|^{-1/2}$. (We use scare quotes to indicate that, since we do not require G to be a group here, the corresponding set of vectors may not be an orbit proper.)

Proof. First, we recall the definition of the shadow norm:

$$\|\Gamma_{\tau}\|_G^2 = \max_{\text{states } \rho} \left(\mathbb{E}_{Q \sim G} \left[\sum_{z \in \{0,1\}^n} \langle z | U(Q) \rho U(Q)^{\dagger} | z \rangle \langle z | U(Q) \mathcal{M}^{-1}(\Gamma_{\tau}) U(Q)^{\dagger} | z \rangle^2 \right] \right). \quad (\text{B21})$$

Adapting Eq. (B15) to the language of frames yields the inequalities

$$\beta_k^{-1} \leq \|\mathcal{M}_G^{-1}(\Gamma_\tau)\| \leq \alpha_k^{-1}, \quad (\text{B22})$$

where we have used the fact that the spectral norm $\|\cdot\|$ of the Majorana operators is 1. Thus

$$\begin{aligned} \|\Gamma_\tau\|_G^2 &\leq \alpha_k^{-2} \max_{\text{states } \rho} \left(\mathbb{E}_{Q \sim G} \left[\sum_{z \in \{0,1\}^n} \langle z | U(Q) \rho U(Q)^\dagger | z \rangle \langle z | U(Q) \Gamma_\tau U(Q)^\dagger | z \rangle^2 \right] \right) \\ &= \alpha_k^{-2} \max_{\text{states } \rho} \left(\mathbb{E}_{Q \sim G} \left[\sum_{z \in \{0,1\}^n} \langle z | U(Q) \rho U(Q)^\dagger | z \rangle \left(\sum_{\mu \in \mathcal{C}_{2n,2k}} \det[(Q^\top)_{\tau,\mu}] \langle z | \Gamma_\mu | z \rangle \right)^2 \right] \right). \end{aligned} \quad (\text{B23})$$

Let us examine the innermost bracketed term. Since $\langle z | \Gamma_\mu | z \rangle = \pm 1$ when $\mu \in \mathcal{D}_{2n,2k}$ and 0 otherwise, we can restrict the sum to run over $\mathcal{D}_{2n,2k}$. Furthermore, by Lemma 3, we know that $\det[(Q^\top)_{\tau,\mu}]$ is nonzero only for one particular μ , which may or may not lie in $\mathcal{D}_{2n,2k}$. This means that the sum contains at most one nonzero term, which takes the value ± 1 , allowing us to “transform” the square into an absolute value:

$$\left(\sum_{\mu \in \mathcal{C}_{2n,2k}} \det[(Q^\top)_{\tau,\mu}] \langle z | \Gamma_\mu | z \rangle \right)^2 = \sum_{\mu \in \mathcal{D}_{2n,2k}} |\det[Q_{\mu,\tau}]|. \quad (\text{B24})$$

Importantly, this quantity does not depend on z , which makes the sum over z trivial (as well as the maximum over all states):

$$\sum_{z \in \{0,1\}^n} \langle z | U(Q) \rho U(Q)^\dagger | z \rangle = \text{tr } \rho = 1. \quad (\text{B25})$$

We are then left with taking the average over $Q \sim G$ in Eq. (B24), which is simply the original quantity of interest obeying the frame bounds [Eq. (B19)]. Therefore

$$\begin{aligned} \|\Gamma_\tau\|_G^2 &\leq \alpha_k^{-2} \mathbb{E}_{Q \sim G} \left[\sum_{\mu \in \mathcal{D}_{2n,2k}} |\det[Q_{\mu,\tau}]| \right] \\ &\leq \alpha_k^{-2} \beta_k. \end{aligned} \quad (\text{B26})$$

To obtain the lower bound, simply reverse the roles of α_k and β_k . Since the only inequalities invoked were those of the frame bounds, it follows that equality holds in both directions if and only if the frame is tight. \square

Lemma 6 is useful in two ways: first, it gives an estimate on the shadow norm for any valid subset of fermionic Gaussian Clifford unitaries, assuming one has bounds on the eigenvalues of \mathcal{M}_G . Second, it tells us that those subsets which give rise to *tight* frames exhibit optimal sample complexity in the sense of the shadow norm. Tight frames generated by the action of finite groups have been completely characterized through representation theory [90, 91]. Below we restate the primary results relevant to our context, which will motivate us to restrict G to a group.

Proposition 8 ([91, Theorems 6.3 and 6.5]). *Let H be a finite group, V a Hilbert space, and $\varphi: H \rightarrow \text{U}(V)$ a unitary representation. Then:*

1. *Every orbit $\varphi(H)v$, $v \in V \setminus \{0\}$, is a tight frame if and only if every orbit spans V [i.e., φ is an irreducible representation (irrep)].*
2. *There exists $v \in V \setminus \{0\}$ for which $\varphi(H)v$ is a tight frame if and only if there exists $w \in V \setminus \{0\}$ such that $\text{span}(\varphi(H)w) = V$.*

In our context, this means that if $\phi_{2k}|_G$ is irreducible, then every orbit is tight, hence saturating the bound of Lemma 6. Alternatively, if $\phi_{2k}|_G$ is not an irrep, there may be only specific orbits which form tight frames. Fortunately, this complication does not arise in our setting due to the fact that we are dealing exclusively with (signed) permutation matrices. We formalize this notion with the following lemma. (Although we are only interested in the even-degree representations, we formulate the statement to apply to all $1 \leq k \leq 2n$ for completeness.)

Lemma 9. Let $G \subseteq \text{Sym}^+(2, 2n)$ be a group such that $\text{span}(\phi_k(G)v_0) = \mathbb{R}^{\binom{2n}{k}}$ for some nonzero $v_0 \in \mathbb{R}^{\binom{2n}{k}}$. Then $\text{span}(\phi_k(G)v) = \mathbb{R}^{\binom{2n}{k}}$ for all nonzero $v \in \mathbb{R}^{\binom{2n}{k}}$.

Proof. Without loss of generality, we can consider v_0 an arbitrary element of the standard basis. From Remark 4, we have $\phi_k(G) \subseteq \text{Sym}[2, \binom{2n}{k}]$; therefore, $\text{span}(\phi_k(G)v_0) = \mathbb{R}^{\binom{2n}{k}}$ if and only if the orbit is the entire basis (modulo signs):

$$\phi_k(G)v_0 = \{e_{\boldsymbol{\mu}} \text{ and/or } -e_{\boldsymbol{\mu}} \mid \boldsymbol{\mu} \in \mathcal{C}_{2n,k}\}. \quad (\text{B27})$$

Now consider some other basis vector $w_0 \neq v_0$. Since there exists some $g \in G$ such that $\phi_k(g)v_0 = \pm w_0$, it follows that

$$\begin{aligned} \phi_k(G)v_0 &= \phi_k(G)[\phi_k(g^{-1})(\pm w_0)] \\ &= \phi_k(Gg^{-1})(\pm w_0) = \phi_k(G)(\pm w_0). \end{aligned} \quad (\text{B28})$$

Since the sign is irrelevant when taking the span, we see that the orbit of any basis vector spans the space. Hence the orbit of every nonzero vector does as well. \square

This result allows us to ignore the second part of Proposition 8, so that we have to consider the irreducibility of $\phi_{2k}|_G$. Furthermore, we do not have to worry about choosing some particular $\boldsymbol{\sigma} \in \mathcal{D}_{2n,2k}$ to generate our cumulative frame; although the specific form of these tuples changes depending on the choice of fermion-to-qubit mapping, the above results tell us that the behavior of such tight frames is uniform across all of $\mathcal{C}_{2n,2k}$.

Enumerating all possible subgroups to search for the one which gives the largest frame bound (hence smallest shadow norm) is a highly impractical task. Fortunately, this is not necessary, as it turns out that *all* irreps $\phi_{2k}|_G$ yield the same frame bound. To see this, we introduce an alternative, equivalent formulation of frames based on the *frame operator* $T: V \rightarrow V$,

$$T := \sum_j \langle x_j, \cdot \rangle x_j, \quad (\text{B29})$$

where $\{x_j\}_j$ is a frame for V .

Proposition 10 ([92, Theorem 3]). *Let H be a finite group, V a Hilbert space, and $\varphi: H \rightarrow \text{U}(V)$ an irreducible unitary representation. For any nonzero $v \in V$, the frame operator for $\varphi(H)v$ is*

$$T = \frac{|\varphi(H)v|}{\dim V} \|v\|_V^2 \mathbb{1}_V, \quad (\text{B30})$$

where $\mathbb{1}_V$ is the identity operator on V .

In general, $T = \alpha \mathbb{1}_V$ if and only if the frame is tight (with frame bound α). In the context of tight frames generated by irreps, this result is essentially a variant on Schur's lemma. The utility of Proposition 10 in particular is that the frame bound is given explicitly. Our claim that all irreducible subgroups yield the same shadow norm then follows.

Theorem 11. *Let $G \subseteq \text{Sym}^+(2, 2n)$ be irreducible with respect to ϕ_{2k} . Then*

$$\begin{aligned} \mathbb{E}_{Q \sim G} \left[\sum_{\boldsymbol{\sigma} \in \mathcal{D}_{2n,2k}} |\det[Q_{\boldsymbol{\sigma}, \boldsymbol{\tau}}]| \right] &\equiv \frac{1}{|G|} \sum_{Q \in G} \sum_{\boldsymbol{\sigma} \in \mathcal{D}_{2n,2k}} |[\phi_{2k}(Q)]_{\boldsymbol{\sigma}\boldsymbol{\tau}}|^2 \\ &= \binom{n}{k} \binom{2n}{2k}^{-1} \end{aligned} \quad (\text{B31})$$

for all $\boldsymbol{\tau} \in \mathcal{C}_{2n,2k}$.

Proof. Consider the orbit $\phi_{2k}(G)(e_{\boldsymbol{\sigma}}|G|^{-1/2})$. Let $\text{Stab}_G(e_{\boldsymbol{\sigma}}) := \{Q \in G \mid \phi_{2k}(Q)e_{\boldsymbol{\sigma}} = e_{\boldsymbol{\sigma}}\}$ be its stabilizer subgroup. By the orbit-stabilizer theorem and Lagrange's theorem [93],

$$|\phi_{2k}(G)(e_{\boldsymbol{\sigma}}|G|^{-1/2})| = \frac{|G|}{|\text{Stab}_G(e_{\boldsymbol{\sigma}})|}. \quad (\text{B32})$$

Using Proposition 10 and recalling that the Hilbert space of our frame is $\mathbb{R}^{\binom{2n}{2k}}$, we see that the corresponding frame bound is

$$\begin{aligned}\alpha_{\sigma} = \|T_{\sigma}\| &= \frac{|G|}{|\text{Stab}_G(e_{\sigma})|} \binom{2n}{2k}^{-1} \left\| \frac{e_{\sigma}}{|G|^{1/2}} \right\|_2^2 \\ &= \frac{1}{|\text{Stab}_G(e_{\sigma})|} \binom{2n}{2k}^{-1}.\end{aligned}\tag{B33}$$

One must be careful when handling this $|\text{Stab}_G(e_{\sigma})|$ term, since, when constructing the frame operator, we sum over all elements of the orbit, rather than of the group. However, the particular sum that we are interested in, namely Eq. (B31), is over the entire group, and thus precisely double counts the elements of the stabilizer subgroup:

$$\begin{aligned}\frac{1}{|G|} \sum_{Q \in G} |[\phi_{2k}(Q)]_{\sigma\tau}|^2 &= \sum_{Q \in G} |\langle \phi_{2k}(Q)^T e_{\sigma} | G|^{-1/2}, e_{\tau} \rangle|^2 \\ &= |\text{Stab}_G(e_{\sigma})| \sum_{w \in \phi_{2k}(G)(e_{\sigma} | G|^{-1/2})} |\langle w, e_{\tau} \rangle|^2 \\ &= |\text{Stab}_G(e_{\sigma})| \alpha_{\sigma} = \binom{2n}{2k}^{-1}.\end{aligned}\tag{B34}$$

Since this quantity does not depend on σ , the remaining sum over $\mathcal{D}_{2n,2k}$ simply incurs a factor of $|\mathcal{D}_{2n,2k}| = \binom{n}{k}$. \square

Corollary 12. *In conjunction with Lemma 6, it immediately follows that*

$$\|\Gamma_{\tau}\|_G^2 = \binom{2n}{2k} \binom{n}{k}^{-1}\tag{B35}$$

for all irreducible $G \subseteq \text{Sym}^+(2, 2n)$.

Finally, in order to obtain a concrete example of such tight frames, we show that $\text{Sym}^+(2, 2n)$ is irreducible with respect to ϕ_k for all $1 \leq k \leq 2n$. Again, though we are only interested in the even-degree case, we prove the statement for general k for completeness. It is then straightforward to show that $\text{Alt}(2n) \subset \text{Sym}^+(2, 2n)$ is also irreducible.

Theorem 13. *Let $G = \text{Sym}^+(2, 2n)$ or $\text{Alt}(2n)$. For all $1 \leq k \leq 2n$, $\phi_k|_G$ is irreducible.*

Proof. We begin with the case $G = \text{Sym}^+(2, 2n)$; it will be apparent that the proof methods adapt fully to the $G = \text{Alt}(2n)$ case. We show irreducibility via a standard result of character theory [94]: $\phi_k|_G$ is an irrep if and only if

$$\frac{1}{|G|} \sum_{Q \in G} \text{tr}[\phi_k(Q)]^2 = 1.\tag{B36}$$

Here, the trace of our representation is simply

$$\text{tr}[\phi_k(Q)] = \sum_{\mu \in \mathcal{C}_{2n,k}} \det[Q_{\mu,\mu}].\tag{B37}$$

Expanding the square yields

$$\frac{1}{|G|} \sum_{Q \in G} \text{tr}[\phi_k(Q)]^2 = \frac{1}{|G|} \sum_{Q \in G} \left(\sum_{\mu \in \mathcal{C}_{2n,k}} \det[Q_{\mu,\mu}]^2 + \sum_{\substack{\mu, \nu \in \mathcal{C}_{2n,k} \\ \mu \neq \nu}} \det[Q_{\mu,\mu}] \det[Q_{\nu,\nu}] \right).\tag{B38}$$

We will calculate the average of the each term separately.

Since $|\det[Q_{\mu,\mu}]| \in \{0, 1\}$, the diagonal sum is

$$\frac{1}{|G|} \sum_{Q \in G} \sum_{\mu \in \mathcal{C}_{2n,k}} \det[Q_{\mu,\mu}]^2 = \sum_{\mu \in \mathcal{C}_{2n,k}} \mathbb{E}_{Q \sim G} |\det[Q_{\mu,\mu}]|.\tag{B39}$$

Intuitively, $\mathbb{E}_{Q \sim G} |\det[Q_{\mu, \mu}]|$ is the “density” of the signed permutation matrices whose (μ, μ) submatrix has nonzero subdeterminant. To compute this average, we proceed by a visual argument using the structure of the matrix. Recall that $\det[Q_{\mu, \mu}] \neq 0$ if and only if $Q_{\mu, \mu} \in \text{Sym}(2, k)$. When writing down a matrix as an array, we can choose any ordering of the row and column indices, so long as this choice is consistent. Therefore, we shall order the indices such that μ lies in the first k rows/columns:

$$Q = \left(\begin{array}{c|c} Q_{\mu, \mu} & * \\ \hline * & * \end{array} \right). \quad (\text{B40})$$

Requiring that $Q_{\mu, \mu} \in \text{Sym}(2, k)$ immediately sets the off-diagonal blocks to be all zeros, hence such a Q is block diagonal in this ordering of rows and columns. Furthermore, since $\det Q = 1$, the remaining $(2n - k) \times (2n - k)$ block must have the same determinant as the $Q_{\mu, \mu}$ block. In other words, a “valid” Q must take the form

$$Q \in \left(\begin{array}{c|c} \text{Sym}^+(2, k) & 0 \\ \hline 0 & \text{Sym}^+(2, 2n - k) \end{array} \right) \cup \left(\begin{array}{c|c} \text{Sym}^-(2, k) & 0 \\ \hline 0 & \text{Sym}^-(2, 2n - k) \end{array} \right), \quad (\text{B41})$$

where $\text{Sym}^-(2, d) := \{R \in \text{Sym}(2, d) \mid \det R = -1\}$. Although $\text{Sym}^-(2, d)$ is not a group, it has the same number of elements as $\text{Sym}^+(2, d)$: $|\text{Sym}^-(2, d)| = |\text{Sym}^+(2, d)| = 2^d d!/2$. The density is thus

$$\begin{aligned} \mathbb{E}_{Q \sim G} |\det[Q_{\mu, \mu}]| &= \frac{|\text{Sym}^+(2, k) \oplus \text{Sym}^+(2, 2n - k)| + |\text{Sym}^-(2, k) \oplus \text{Sym}^-(2, 2n - k)|}{|\text{Sym}^+(2, 2n)|} \\ &= \frac{2(2^k k! 2^{2n-k} (2n - k)!)/4}{2^{2n} (2n)!/2} = \binom{2n}{k}^{-1}, \end{aligned} \quad (\text{B42})$$

and so

$$\sum_{\mu \in \mathcal{C}_{2n, k}} \mathbb{E}_{Q \sim G} |\det[Q_{\mu, \mu}]| = 1. \quad (\text{B43})$$

Next we show that the off-diagonal sum of Eq. (B38) vanishes. The argument follows by generalizing the above calculation. For $\mu \neq \nu$, the tuples (thought of as sets) may overlap $j \in \{0, \dots, k - 1\}$ times. We order the matrix representation such that μ makes up the first k rows/columns as before, but additionally the overlapping indices $\mu \cap \nu$ are placed at the last j spots of this $k \times k$ block. We then place the remaining part of ν in the following $(k - j) \times (k - j)$ block. Visually, we have

$$Q = \left(\begin{array}{c|c|c|c} Q_{\mu \setminus \nu, \mu \setminus \nu} & 0 & 0 & 0 \\ \hline 0 & Q_{\mu \cap \nu, \mu \cap \nu} & 0 & 0 \\ \hline 0 & 0 & Q_{\nu \setminus \mu, \nu \setminus \mu} & 0 \\ \hline 0 & 0 & 0 & * \end{array} \right), \quad (\text{B44})$$

where the lengths of the four blocks are $k - j$, j , $k - j$, and $2(n - k) + j$, respectively. If either $\det[Q_{\mu, \mu}]$ or $\det[Q_{\nu, \nu}]$ are 0, then that term in the sum trivially vanishes. Thus consider the case in which they are both nonzero. Again, since we have the constraint $\det Q = 1$, the product of the determinants of all four blocks must be 1. There are eight cases in which $\det[Q_{\mu, \mu}] \det[Q_{\nu, \nu}] \neq 0$: $Q \in \text{Sym}^a(2, k - j) \oplus \text{Sym}^b(2, j) \oplus \text{Sym}^c(2, k - j) \oplus \text{Sym}^d(2, 2(n - k) + j)$, where

$$(a, b, c, d) \in \left\{ (+, +, +, +), (+, +, -, -), (+, -, +, -), (+, -, -, +), (-, +, +, -), (-, +, -, +), (-, -, +, +), (-, -, -, -) \right\}. \quad (\text{B45})$$

With this formalism, we can read off the terms in the off-diagonal sum as $\det[Q_{\mu, \mu}] \det[Q_{\nu, \nu}] = (ab)(bc) = ac$ (where our notation means $a = \pm \equiv \pm 1$, etc.). By examining Eq. (B45), we see that four of the possibilities give $ac = +1$, while the other four give $ac = -1$. Since the number of elements in each of the eight subsets are all the same, exactly half the terms in the sum will cancel with the other half, hence

$$\sum_{Q \in G} \det[Q_{\mu, \mu}] \det[Q_{\nu, \nu}] = 0 \quad \forall \mu \neq \nu \quad (\text{B46})$$

as desired.

Thus,

$$\frac{1}{|G|} \sum_{Q \in G} \text{tr}[\phi_k(Q)]^2 = 1, \quad (\text{B47})$$

and so $\phi_k|_G$ is irreducible.

The proof readily adapts for $G = \text{Alt}(2n)$. As we saw in Eq. (B42), the fact that the matrix elements have signs is irrelevant, as the factors arising due to the wreath product (i.e., 2^k , 2^{2n-k} , and 2^{2n}) exactly cancel out. One may then simply replace every appearance of $\text{Sym}^+(2, d)$ with $\text{Sym}^+(d) \equiv \text{Alt}(d)$ and $\text{Sym}^-(2, d)$ with $\text{Sym}^-(d)$ without consequence. \square

In conjunction with the rigorous guarantees of classical shadows, Theorem 1 of the main text follows. Note that we use Stirling's approximation to simplify the shadow norm expression, and that

$$\log \left(\sum_{j=1}^k |\mathcal{C}_{2n,2j}| \right) = \mathcal{O}(k \log n). \quad (\text{B48})$$

3. The classical shadow estimator

Here we provide a derivation for the formal expressions of the linear inversion estimator used in the classical shadows methodology. Recalling Eq. (B6), and using the linearity of $\mathcal{M}_{\text{FGU}}^{-1}$, the classical shadow is simply

$$\begin{aligned} \hat{\rho}_{Q,z} &\equiv \mathcal{M}_{\text{FGU}}^{-1}(U(Q)^\dagger |z\rangle\langle z|U(Q)) \\ &= \frac{1}{2^n} \left(\mathbb{1} + \sum_{j=1}^n \lambda_{n,j}^{-1} \sum_{\mu \in \mathcal{D}_{2n,2j}} \langle z | \Gamma_\mu | z \rangle \sum_{\nu \in \mathcal{C}_{2n,2j}} \det[Q_{\mu,\nu}] \Gamma_\nu \right), \end{aligned} \quad (\text{B49})$$

where $\lambda_{n,j}^{-1} = \binom{2n}{2j} / \binom{n}{j}$. Passing this expression into the expectation value estimator, we then obtain

$$\begin{aligned} \text{tr}(\Gamma_\tau \hat{\rho}_{Q,z}) &= \frac{1}{2^n} \left(\text{tr}(\Gamma_\tau) + \sum_{j=1}^n \lambda_{n,j}^{-1} \sum_{\mu \in \mathcal{D}_{2n,2j}} \langle z | \Gamma_\mu | z \rangle \sum_{\nu \in \mathcal{C}_{2n,2j}} \det[Q_{\mu,\nu}] \text{tr}(\Gamma_\tau \Gamma_\nu) \right) \\ &= \lambda_{n,k}^{-1} \sum_{\mu \in \mathcal{D}_{2n,2k}} \langle z | \Gamma_\mu | z \rangle \det[Q_{\mu,\tau}] \end{aligned} \quad (\text{B50})$$

for all $\tau \in \mathcal{C}_{2n,2k}$.

4. Expressions for arbitrary observables

For completeness, we demonstrate how to compute the shadow norm (and hence the estimator variance) of an arbitrary fermionic observable. This result will be particularly useful in the context of Hamiltonian averaging (Appendix E 3).

Any element of $\mathcal{A}_{\text{even}}^{(n)}$ can be written as

$$O = h_\emptyset \mathbb{1} + \sum_{k=1}^n \sum_{\mu \in \mathcal{C}_{2n,2k}} h_\mu \Gamma_\mu, \quad (\text{B51})$$

where $h_\mu \in \mathbb{R}$. Without loss of generality, we shall take $\text{tr} O = 0$, since the identity component is irrelevant for variance calculations.

We begin with the familiar expression

$$\mathcal{M}_{\text{FGU}}^{-1}(O) = \sum_{k=1}^n \lambda_{n,k}^{-1} \sum_{\mu \in \mathcal{C}_{2n,2k}} h_\mu \Gamma_\mu. \quad (\text{B52})$$

From this we write

$$\begin{aligned} \langle z|U(Q)\mathcal{M}_{\text{FGU}}^{-1}(O)U(Q)^\dagger|z\rangle^2 &= \left(\sum_{k=1}^n \lambda_{n,k}^{-1} \sum_{\mu \in \mathcal{C}_{2n,2k}} h_\mu \sum_{\nu \in \mathcal{D}_{2n,2k}} \det[Q_{\nu,\mu}] \langle z|\Gamma_\nu|z\rangle \right)^2 \\ &= \sum_{k,k'=1}^n \sum_{\substack{\mu \in \mathcal{C}_{2n,2k} \\ \mu' \in \mathcal{C}_{2n,2k'}}} \sum_{\substack{\nu \in \mathcal{D}_{2n,2k} \\ \nu' \in \mathcal{D}_{2n,2k'}}} \lambda_{n,k}^{-1} \lambda_{n,k'}^{-1} h_\mu h_{\mu'} \det[Q_{\nu,\mu}] \det[Q_{\nu',\mu'}] \langle z|\Gamma_\nu|z\rangle \langle z|\Gamma_{\nu'}|z\rangle, \end{aligned} \quad (\text{B53})$$

where recall that $Q \in \text{Alt}(2n)$.

For the state-dependent probability factor, we first write the state ρ in its most general form:

$$\rho = \frac{1}{2^n} \left(\mathbb{1} + \sum_{j=1}^{2n} \sum_{\tau \in \mathcal{C}_{2n,j}} g_\tau \Gamma_\tau \right), \quad (\text{B54})$$

where $g_\tau = \text{tr}(\Gamma_\tau \rho) \in \mathbb{R}$. Then its rotated diagonal matrix elements are

$$\langle z|U(Q)\rho U(Q)^\dagger|z\rangle = \frac{1}{2^n} \left(1 + \sum_{j=1}^n \sum_{\tau \in \mathcal{C}_{2n,2j}} g_\tau \sum_{\sigma \in \mathcal{D}_{2n,2j}} \det[Q_{\sigma,\tau}] \langle z|\Gamma_\sigma|z\rangle \right). \quad (\text{B55})$$

Note that only the support over $\mathcal{A}_{\text{even}}^{(n)}$ remains, since the odd-degree terms all have vanishing diagonal matrix elements.

Next we multiply Eqs. (B53) and (B55) and sum over $z \in \{0,1\}^n$. Observe that there are only two types of terms in this sum which depend on z :

$$\sum_{z \in \{0,1\}^n} \langle z|\Gamma_\nu|z\rangle \langle z|\Gamma_{\nu'}|z\rangle = \text{tr}(\Gamma_\nu \Gamma_{\nu'}) = 2^n \delta_{\nu\nu'}, \quad (\text{B56})$$

$$\sum_{z \in \{0,1\}^n} \langle z|\Gamma_\sigma|z\rangle \langle z|\Gamma_\nu|z\rangle \langle z|\Gamma_{\nu'}|z\rangle = \text{tr}(\Gamma_\sigma \Gamma_\nu \Gamma_{\nu'}) = 0. \quad (\text{B57})$$

Thus, just as we saw in the calculation of the shadow norm for individual Majorana operators, the details of the state do not come into play here—only the trivial fact that $\text{tr } \rho = 1$ matters. We then have

$$\begin{aligned} &\mathbb{E}_{Q \sim \text{Alt}(2n)} \left[\sum_{z \in \{0,1\}^n} \langle z|U(Q)\rho U(Q)^\dagger|z\rangle \langle z|U(Q)\mathcal{M}^{-1}(H)U(Q)^\dagger|z\rangle^2 \right] \\ &= \mathbb{E}_{Q \sim \text{Alt}(2n)} \left[\frac{1}{2^n} \sum_{k,k'=1}^n \sum_{\substack{\mu \in \mathcal{C}_{2n,2k} \\ \mu' \in \mathcal{C}_{2n,2k'}}} \sum_{\substack{\nu \in \mathcal{D}_{2n,2k} \\ \nu' \in \mathcal{D}_{2n,2k'}}} \lambda_{n,k}^{-1} \lambda_{n,k'}^{-1} h_\mu h_{\mu'} \det[Q_{\nu,\mu}] \det[Q_{\nu',\mu'}] 2^n \delta_{\nu\nu'} \right] \\ &= \sum_{k=1}^n \sum_{\mu, \mu' \in \mathcal{C}_{2n,2k}} \lambda_{n,k}^{-2} h_\mu h_{\mu'} \mathbb{E}_{Q \sim \text{Alt}(2n)} \left[\sum_{\nu \in \mathcal{D}_{2n,2k}} \det[Q_{\nu,\mu}] \det[Q_{\nu,\mu'}] \right]. \end{aligned} \quad (\text{B58})$$

From Lemma 3, $\det[Q_{\nu,\mu}] \det[Q_{\nu,\mu'}] = |\det[Q_{\nu,\mu}]| \delta_{\mu\mu'}$, and so the above ensemble average is simply the channel eigenvalue $\lambda_{n,k}$ once again (Theorem 11). Altogether, we arrive at

$$\begin{aligned} \|O\|_{\text{FGU}}^2 &= \sum_{k=1}^n \sum_{\mu \in \mathcal{C}_{2n,2k}} \|h_\mu \Gamma_\mu\|_{\text{FGU}}^2 \\ &= \sum_{k=1}^n \lambda_{n,k}^{-1} \sum_{\mu \in \mathcal{C}_{2n,2k}} h_\mu^2. \end{aligned} \quad (\text{B59})$$

This result implies that the shadow norm here behaves as a 2-norm over $\mathcal{A}_{\text{even}}^{(n)}$, with the Majorana operators serving as an unnormalized (with respect to $\|\cdot\|_{\text{FGU}}$) basis. Furthermore, from the details of these calculations, we see that the shadow norm is naturally state-independent in this case. Thus the exact expression for this variance is

$$\text{Var}_{Q,z}[\text{tr}(O\hat{\rho}_{Q,z})] = \sum_{k=1}^n \lambda_{n,k}^{-1} \sum_{\mu \in \mathcal{C}_{2n,2k}} h_\mu^2 - \text{tr}(O\rho)^2. \quad (\text{B60})$$

5. Performance guarantees without median-of-means estimation

As remarked in the main text, we do not require the median-of-means technique proposed in the original work [38] to obtain the same rigorous sampling bounds. Instead, one may simply use standard estimation via means: given M independently obtained classical shadows $\hat{\rho}_1, \dots, \hat{\rho}_M$, define

$$\omega_j(M) := \frac{1}{M} \sum_{i=1}^M \text{tr}(O_j \hat{\rho}_i) \quad (\text{B61})$$

for each $j \in \{1, \dots, L\}$. Below, we state a general condition in which this estimator yields sample complexity equivalent to that of the median-of-means estimator.

Theorem 14. *Suppose the classical shadow estimators $\hat{\rho}_{U,z}$ satisfy*

$$-\|O_j\|_{\mathcal{U}}^2 \leq \text{tr}(O_j \hat{\rho}_{U,z}) \leq \|O_j\|_{\mathcal{U}}^2 \quad (\text{B62})$$

for all $U \in \mathcal{U}$, $z \in \{0, 1\}^n$, and $j \in \{1, \dots, L\}$. Then by setting $\delta \in (0, 1)$,

$$M = \frac{2 \log(2L/\delta)}{\varepsilon^2} \max_{1 \leq j \leq L} \|O_j\|_{\mathcal{U}}^2, \quad (\text{B63})$$

all mean-value estimators $\omega_1(M), \dots, \omega_L(M)$ satisfy

$$|\omega_j(M) - \text{tr}(O_j \rho)| \leq \varepsilon, \quad (\text{B64})$$

with probability at least $1 - \delta$.

Proof. The claim follows straightforwardly from Hoeffding's inequality [77], which states that for a collection of independent random variables X_1, \dots, X_M bounded by the intervals $[a_i, b_i]$ for each $i \in \{1, \dots, M\}$, the probability that their sample mean $\bar{X} := \frac{1}{M} \sum_{i=1}^M X_i$ deviates from the true mean $\mathbb{E}[\bar{X}]$ by more than ε is bounded as

$$\Pr[|\bar{X} - \mathbb{E}[\bar{X}]| \geq \varepsilon] \leq 2 \exp\left(-\frac{2M^2\varepsilon^2}{\sum_{i=1}^M (b_i - a_i)^2}\right). \quad (\text{B65})$$

In our setting, for each $j \in \{1, \dots, L\}$, we have $\bar{X} = \omega_j(M)$ and $b_i = -a_i = \|O_j\|_{\mathcal{U}}^2$ for all $1 \leq i \leq M$. The concentration inequality then reads

$$\Pr[|\omega_j(M) - \text{tr}(O_j \rho)| \geq \varepsilon] \leq 2 \exp\left(-\frac{2M\varepsilon^2}{4\|O_j\|_{\mathcal{U}}^2}\right). \quad (\text{B66})$$

If we require that each probability of failure be no more than δ/L , then from a union bound over all L events, we can succeed with probability at least $1 - \delta$ by setting

$$2 \exp\left(-\frac{M\varepsilon^2/2}{\max_{1 \leq j \leq L} \|O_j\|_{\mathcal{U}}^2}\right) = \frac{\delta}{L}. \quad (\text{B67})$$

Solving for M yields Eq. (B63). □

Note that we achieve optimal scaling with the failure parameter δ , which was one of the advantages of median-of-means in the general case. Obvious generalizations of this result also follow by modifying Eq. (B62) (e.g., multiplying the bounds by arbitrary constant factors). For our purposes, however, the classical shadow estimators with $\mathcal{U} = \mathcal{U}_{\text{FGU}}$ precisely obey the bounds as presented when taking the observables as Majorana operators, as is evident from Eq. (B50). In fact, the Pauli-basis measurements ($\mathcal{U} = \text{Cl}(1)^{\otimes n}$) also satisfy this condition when applied strictly to Pauli observables. However, this does not necessarily hold for arbitrary observables, nor for arbitrary ensembles.

Interestingly, Eq. (B63) features significantly smaller numerical factors than what is obtained from the median-of-means approach, although we recognize that the proof techniques presented in Ref. [38] were not particularly optimized in this regard.

Appendix C: Computations with the number-conserving modification

We now prove Theorem 2 of the main text. Many of the techniques used here follow straightforwardly from the fermionic formalism developed in Appendix B, along with the tools used to study the single-qubit Clifford ensemble in the original work on classical shadows [38]. In Appendix C 1, we first evaluate the channel \mathcal{M}_{NC} [which again is diagonalized by the Majorana operators; Eq. (C5)] and provide an expression for its eigenvalues/shadow norm [Eq. (C7)]. Then, recognizing that generically do not possess a closed-form expression, in Appendix C 2 we obtain an upper bound on the shadow norm for this ensemble, which is asymptotically optimal [Eq. (C22)].

For ease of notation, with $u \in \text{Sym}(n)$, we shall write $U(u)^\dagger a_p U(u) = a_{u(p)}$, where $u(p)$ is understood in the sense of the action of the permutation u on the mode indices $\{0, \dots, n-1\}$. We further generalize this notation to act on $\{0, \dots, 2n-1\}$, in accordance with the definition of Majorana operators. Consider $\mu \in \mathcal{C}_{2n,k}$, where each index takes the form $\mu_j = 2q_j + x_j$ for $q_j \in \{0, 2, \dots, 2n-4, 2n-2\}$ and $x_j \in \{0, 1\}$. We define $\tilde{u}(\mu) := (2u(q_1) + x_1, \dots, 2u(q_k) + x_k)$, so that $U(u)^\dagger \Gamma_\mu U(u) = \Gamma_{\tilde{u}(\mu)}$. Note that $\tilde{u}(\mu)$ is not necessarily ordered monotonically, so $\Gamma_{\tilde{u}(\mu)}$ may differ from our standard definition of the Majorana operators by a minus sign. This detail is irrelevant to our present analysis, so we shall ignore it.

1. The shadow norm

The ensemble we consider here is

$$\mathcal{U}_{\text{NC}} = \{V \circ U(u) \mid V \in \text{Cl}(1)^{\otimes n}, u \in \text{Alt}(n)\}. \quad (\text{C1})$$

We wish to evaluate the following expression for the classical shadows channel:

$$\begin{aligned} \mathcal{M}_{\text{NC}}(\Gamma_\mu) &= \mathbb{E}_{\substack{V \sim \text{Cl}(1)^{\otimes n} \\ u \sim \text{Alt}(n)}} \left[\sum_{z \in \{0,1\}^n} \langle z | V U(u) \Gamma_\mu U(u)^\dagger V^\dagger | z \rangle U(u)^\dagger V^\dagger | z \rangle \langle z | V U(u) \right] \\ &= \mathbb{E}_{u \sim \text{Alt}(n)} \left[U(u)^\dagger \sum_{z \in \{0,1\}^n} \mathbb{E}_{V \sim \text{Cl}(1)^{\otimes n}} \left[\langle z | V \Gamma_{\tilde{u}^{-1}(\mu)} V^\dagger | z \rangle V^\dagger | z \rangle \langle z | V \right] U(u) \right]. \end{aligned} \quad (\text{C2})$$

The average over $\text{Cl}(1)^{\otimes n}$ is precisely the same quantity evaluated in Ref. [38]. For convenience, we restate their results here: let $|x\rangle = |x_1\rangle \otimes \dots \otimes |x_n\rangle$ be a product state over n qubits and A, B, C be Hermitian matrices which decompose into the same tensor product structure, $A = A_1 \otimes \dots \otimes A_n$, etc. Then

$$\mathbb{E}_{V \sim \text{Cl}(1)^{\otimes n}} [V^\dagger |x\rangle \langle x| V \langle x| V A V^\dagger |x\rangle] = \bigotimes_{j=1}^n \left(\frac{A_j + \text{tr}(A_j)I}{6} \right), \quad (\text{C3})$$

and for each j such that $\text{tr } B_j = \text{tr } C_j = 0$,

$$\mathbb{E}_{V_j \sim \text{Cl}(1)} [V_j^\dagger |x_j\rangle \langle x_j| V_j \langle x_j| V_j B_j V_j^\dagger |x_j\rangle \langle x_j| V_j C_j V_j^\dagger |x_j\rangle] = \frac{B_j C_j + C_j B_j + \text{tr}(B_j C_j)I}{24}. \quad (\text{C4})$$

To understand the tensor product structure of Majorana operators, we must fix some qubit mapping. Understanding $\Gamma_{\tilde{u}^{-1}(\mu)}$ as a Pauli operator under such a mapping, we use Eq. (C3) to obtain

$$\begin{aligned} \mathcal{M}_{\text{NC}}(\Gamma_\mu) &= \mathbb{E}_{u \sim \text{Alt}(n)} \left[\frac{1}{3^{\text{loc}(\Gamma_{\tilde{u}^{-1}(\mu)})}} U(u)^\dagger \Gamma_{\tilde{u}^{-1}(\mu)} U(u) \right] \\ &= \mathbb{E}_{u \sim \text{Alt}(n)} \left[\frac{1}{3^{\text{loc}(\Gamma_{\tilde{u}^{-1}(\mu)})}} \right] \Gamma_\mu, \end{aligned} \quad (\text{C5})$$

where $\text{loc}(\Gamma_{\tilde{u}^{-1}(\mu)})$ is the qubit locality of $\Gamma_{\tilde{u}^{-1}(\mu)}$. Since $u \mapsto u^{-1}$ is a bijection, we may equivalently express the average over $\text{Alt}(n)$ using $\tilde{u}(\mu)$ rather than its inverse.

Let λ_{μ} be the eigenvalues of \mathcal{M}_{NC} , given above in Eq. (C5). For the calculation of the shadow norm, we have

$$\begin{aligned} \|\Gamma_{\mu}\|_{\text{NC}}^2 &= \max_{\substack{\text{states } \rho \\ u \sim \text{Alt}(n)}} \left(\mathbb{E}_{V \sim \text{Cl}(1)^{\otimes n}} \left[\sum_{z \in \{0,1\}^n} \langle z | VU(u)\rho U(u)^\dagger V^\dagger | z \rangle \langle z | VU(u)\mathcal{M}^{-1}(\Gamma_{\mu})U(u)^\dagger V^\dagger | z \rangle^2 \right] \right), \\ &= \lambda_{\mu}^{-2} \max_{\substack{\text{states } \rho \\ u \sim \text{Alt}(n)}} \left(\mathbb{E}_{u \sim \text{Alt}(n)} \left[\text{tr} \left(U(u)^\dagger \rho U(u) \sum_{z \in \{0,1\}^n} \mathbb{E}_{V \sim \text{Cl}(1)^{\otimes n}} [V^\dagger | z \rangle \langle z | V \langle z | V \Gamma_{\tilde{u}^{-1}(\mu)} V^\dagger | z \rangle^2] \right) \right] \right). \end{aligned} \quad (\text{C6})$$

We then use Eq. (C3) to evaluate the Clifford average over the identity factors of $\Gamma_{\tilde{u}^{-1}(\mu)}$, and Eq. (C4) for the nontrivial factors:

$$\begin{aligned} \|\Gamma_{\mu}\|_{\text{NC}}^2 &= \lambda_{\mu}^{-2} \max_{\substack{\text{states } \rho \\ u \sim \text{Alt}(n)}} \left(\mathbb{E}_{u \sim \text{Alt}(n)} \left[\text{tr} \left(U(u)^\dagger \rho U(u) \frac{1}{3^{\text{loc}(\Gamma_{\tilde{u}^{-1}(\mu)})}} \right) \right] \right) \\ &= \lambda_{\mu}^{-1}. \end{aligned} \quad (\text{C7})$$

2. Universal upper bounds on the shadow norm

Although there is no closed-form expression for λ_{μ}^{-1} , we can still obtain a nontrivial estimate for it. To do so, we will evaluate the qubit locality with respect to the Jordan–Wigner transformation. This serves as a universal upper bound for all encodings, since the Jordan–Wigner mapping is maximally nonlocal. We formalize this notion with Jensen’s inequality: since $x \mapsto 3^{-x}$ is concave, we have that

$$\mathbb{E}_{u \sim \text{Alt}(n)} [3^{-\text{loc}(\Gamma_{\tilde{u}(\mu)})}] \geq 3^{-\mathbb{E}_{u \sim \text{Alt}(n)} [\text{loc}(\Gamma_{\tilde{u}(\mu)})]}, \quad (\text{C8})$$

where $\text{loc}(\cdot)$ is with respect to any arbitrary encoding. Then let $\text{loc}_{\text{JW}}(\cdot)$ be the qubit locality specifically under the Jordan–Wigner transformation. Since it is maximally nonlocal, so is its average locality (over a fixed fermionic degree of $2k$), and hence

$$\max_{\mu \in \mathcal{C}_{2n,2k}} \lambda_{\mu}^{-1} \leq \max_{\mu \in \mathcal{C}_{2n,2k}} 3^{\mathbb{E}_{u \sim \text{Alt}(n)} [\text{loc}(\Gamma_{\tilde{u}(\mu)})]} \leq \max_{\mu \in \mathcal{C}_{2n,2k}} 3^{\mathbb{E}_{u \sim \text{Alt}(n)} [\text{loc}_{\text{JW}}(\Gamma_{\tilde{u}(\mu)})]}. \quad (\text{C9})$$

Thus for the rest of this section, all notions of qubit locality will be understood with respect to the Jordan–Wigner transformation exclusively.

Since the qubit locality of Majorana operators varies within a given $\mathcal{C}_{2n,2k}$, we obtain an upper bound by considering the most nonlocal $2k$ -degree operators. Fortunately, under Jordan–Wigner it is simple to identify such operators. Let $W \in \{X, Y\}$ and $\mathbf{q} \in \mathcal{C}_{n,2k}$; maximum locality is achieved by operators of the form

$$P_{\mathbf{q}} := \prod_{i=1}^k W_{q_{2i-1}} Z_{q_{2i-1}+1} \cdots Z_{q_{2i}-1} W_{q_{2i}}, \quad (\text{C10})$$

$$\text{loc}(P_{\mathbf{q}}) = \sum_{i=1}^k (q_{2i} - q_{2i-1} + 1). \quad (\text{C11})$$

Note that we require $n \geq 2k$ for such a Pauli operator to exist. (For the fringe cases in which $n < 2k$, since we are evaluating an upper bound, the final result still holds.)

By applying a permutation u on \mathbf{q} , one changes this locality by reducing or lengthening the various “Jordan–Wigner strings” of Pauli- Z operators in between each pair (q_{2i-1}, q_{2i}) . Observe that $\text{loc}(P_{\mathbf{q}}) \in \{2k, \dots, n\}$. Therefore, if we can calculate the number of permutations which correspond to each level of locality, we may compute

$$\mathbb{E}_{u \sim \text{Alt}(n)} [3^{-\text{loc}(P_{u(\mathbf{q})})}] = \frac{2}{n!} \sum_{\ell=2k}^n 3^{-\ell} |\{u \in \text{Alt}(n) \mid \text{loc}(P_{u(\mathbf{q})}) = \ell\}|. \quad (\text{C12})$$

We determine the size of this set in three steps. First, for a given configuration $u(\mathbf{q})$, we count the number of equivalent permutations which give the same Pauli operator, modulo signs. These permutations merely reorder the $2k$ relevant

indices and the $n - 2k$ remaining indices independently. Accounting for the fact that the entire permutation must be even parity, we have

$$\begin{aligned} |\text{Alt}(2k) \oplus \text{Alt}(n - 2k)| + |\text{Sym}^-(2k) \oplus \text{Sym}^-(n - 2k)| &= \frac{(2k)!}{2} \frac{(n - 2k)!}{2} + \frac{(2k)!}{2} \frac{(n - 2k)!}{2} \\ &= \frac{(2k)!(n - 2k)!}{2} \end{aligned} \quad (\text{C13})$$

such permutations. With this factor at hand, we now only need to consider unique combinations of indices—that is, we assume $u(q_1) < \dots < u(q_{2k})$ in the sequel.

Next, we calculate how many configurations of Jordan–Wigner strings give rise to a qubit locality of exactly ℓ . Let $l_i := u(q_{2i}) - u(q_{2i-1}) > 0$. This problem is equivalent to finding all k -tuples (l_1, \dots, l_k) of positive integers such that

$$\sum_{i=1}^k (l_i + 1) = \ell. \quad (\text{C14})$$

This is an instance of the classic “stars-and-bars” combinatorial problem, wherein we wish to fit $\ell - k$ objects into k bins such that each bin has at least 1 object. There are $\binom{\ell-k-1}{k-1}$ ways to do so.

Finally, we need to account for the $n - \ell$ remaining indices which were not fixed by Eq. (C14). These indices correspond to the qubits *outside* of the Jordan–Wigner strings, i.e., on which $P_{u(\mathbf{q})}$ acts trivially. By a similar combinatorial argument, there are a total of $k + 1$ such spaces to place these trivial indices, of which we may select $j \in \{1, \dots, k + 1\}$. Again we use the stars-and-bars argument: there are $n - \ell$ objects we wish to place into j bins, which can be accomplished in $\binom{n-\ell-1}{j-1}$ unique ways. Summing over all possible values of j gives us

$$\begin{aligned} \sum_{j=1}^{k+1} \binom{k+1}{j} \binom{n-\ell-1}{j-1} &= \sum_{j=1}^{k+1} \binom{k+1}{k+1-j} \binom{n-\ell-1}{j-1} \\ &= \sum_{j=0}^k \binom{k+1}{k-j} \binom{n-\ell-1}{j} = \binom{n+k-\ell}{k} \end{aligned} \quad (\text{C15})$$

different combinations of the $n - \ell$ trivial indices. Note that the Chu–Vandermonde identity was applied to evaluate the sum in the final line.

Reconciling the three steps of our calculation, we obtain

$$|\{u \in \text{Sym}(n) \mid \text{loc}(P_{u(\mathbf{q})}) = \ell\}| = (2k)!(n - 2k)! \binom{\ell - k - 1}{k - 1} \binom{n + k - \ell}{k}, \quad (\text{C16})$$

and so Eq. (C12) can be expressed as

$$\begin{aligned} \mathbb{E}_{u \sim \text{Sym}(n)} \left[3^{-\text{loc}(P_{u(\mathbf{q})})} \right] &= \frac{1}{n!} \sum_{\ell=2k}^n 3^{-\ell} |\{u \in \text{Sym}(n) \mid \text{loc}(P_{u(\mathbf{q})}) = \ell\}| \\ &= \frac{(2k)!(n - 2k)!}{n!} \sum_{\ell=2k}^n 3^{-\ell} \binom{\ell - k - 1}{k - 1} \binom{n + k - \ell}{k}. \end{aligned} \quad (\text{C17})$$

To evaluate this sum, first we relabel the index ℓ to run from 0 to $n - 2k$, so that the summand becomes $3^{-(\ell+2k)} \binom{\ell+k-1}{k-1} \binom{n-k-\ell}{k}$. Using the combinatorial identity

$$\binom{n-k}{\ell} \binom{n-k-\ell}{k} = \binom{n-k}{k} \binom{n-2k}{\ell}, \quad (\text{C18})$$

we have

$$\begin{aligned} \binom{n-k-\ell}{k} &= \binom{n-k}{k} \frac{(n-2k)!}{(n-2k-\ell)!\ell!} \frac{(n-k-\ell)!\ell!}{(n-k)!} \\ &= \binom{n-k}{k} \frac{(2k-n)_\ell}{(k-n)_\ell}, \end{aligned} \quad (\text{C19})$$

where $(m)_\ell := \prod_{j=0}^{n-1} (m+j)$ is the rising Pochhammer symbol. We recognize that the other binomial coefficient can also be expressed using these Pochhammer symbols:

$$\binom{\ell+k-1}{k-1} = \frac{(k)_\ell}{\ell!}. \quad (\text{C20})$$

The sum can therefore be understood in terms of the Gauss hypergeometric function ${}_2F_1$:

$$\begin{aligned} \mathbb{E}_{u \sim \text{Sym}(n)} \left[3^{-\text{loc}(P_{u(\mathbf{q})})} \right] &= \binom{n}{2k}^{-1} \binom{n-k}{k} 9^{-k} \sum_{\ell=0}^{n-2k} \frac{3^{-\ell}}{\ell!} \frac{(k)_\ell (2k-n)_\ell}{(k-n)_\ell} \\ &= \binom{n}{2k}^{-1} \binom{n-k}{k} 9^{-k} {}_2F_1(k, 2k-n; k-n; 1/3). \end{aligned} \quad (\text{C21})$$

Using standard properties of the hypergeometric function, for n and k being positive integers and k a constant, we have the bounds $1 \leq {}_2F_1(k, 2k-n; k-n; 1/3) \leq (3/2)^k$. In particular, this factor is independent of n .

We are ultimately interested in the lower bound of Eq. (C21), since the shadow norm is its reciprocal. Then for $k = \mathcal{O}(1)$, we obtain

$$\|P_{\mathbf{q}}\|_{\text{NC}}^2 \leq \binom{n}{2k} \binom{n-k}{k}^{-1} 9^k = \mathcal{O}(n^k). \quad (\text{C22})$$

Appendix D: Fermionic swap network bounds

In this section we describe another strategy to measure the k -RDM with almost optimal scaling in n . Generalizing from the measurement scheme introduced in Ref. [54] for 1-RDMs, this scheme employs fermionic swap gates to relabel which qubits correspond to which orbitals such that each k -RDM observable becomes a $2k$ -local qubit observable. These local qubit observables may then be measured in a parallel fashion via Pauli measurements. As the circuit structure is equivalent, our \mathcal{U}_{NC} -based scheme may be viewed as a randomized version of this strategy.

For simplicity, we employ the Jordan–Wigner encoding throughout this section. The use of fermionic swap networks to minimize the qubit locality of fermionic operators was first utilized in the context of Hamiltonian simulation [79].

1. The 1-RDM method

We briefly describe the methods of Ref. [54] here. Consider estimating the 1-RDM elements $\text{tr}(a_p^\dagger a_q \rho)$. The observables here are $\frac{1}{2}(a_p^\dagger a_q + \text{h.c.})$ and $\frac{1}{2i}(a_p^\dagger a_q - \text{h.c.})$, corresponding to the real and imaginary parts of the RDM element. In the experiment of Ref. [54], they implement unitaries such that the imaginary part vanishes; for full generality, we will keep the imaginary parts. Diagonal elements are trivial to measure, since

$$a_p^\dagger a_p = \frac{I - Z_p}{2}. \quad (\text{D1})$$

The one-off-diagonal terms are precisely the local qubit operators we are interested in:

$$\frac{a_p^\dagger a_{p+1} + a_{p+1}^\dagger a_p}{2} = \frac{X_p X_{p+1} + Y_p Y_{p+1}}{4}, \quad (\text{D2})$$

$$\frac{a_p^\dagger a_{p+1} - a_{p+1}^\dagger a_p}{2i} = \frac{X_p Y_{p+1} - Y_p X_{p+1}}{4}. \quad (\text{D3})$$

Consider even and odd pairs of orbitals—even pairs being those starting with even indices, and analogously for the odd pairs. For the expectation values $\text{tr}(a_p^\dagger a_{p+1} \rho)$ on even pairs, we measure in 4 different bases: X on all qubits, Y on all qubits, X on every even qubit and Y on every odd qubit, and vice versa. Formally, the observables we measure are

$$\begin{aligned} O_1 &= \prod_{p=0}^{n-1} X_p, & O_2 &= \prod_{p=0}^{n-1} Y_p \\ O_3 &= \prod_{\substack{p=0 \\ \text{even}}}^{n-2} X_p Y_{p+1}, & O_4 &= \prod_{\substack{p=0 \\ \text{even}}}^{n-2} Y_p X_{p+1}. \end{aligned} \quad (\text{D4})$$

If n is odd, then we simply ignore the final Y (resp. X) in O_3 (resp. O_4).

The remaining off-diagonal elements will incur Jordan–Wigner strings, making the Pauli operators highly nonlocal. To circumvent this, we perform fermionic swaps to relabel the indices such that we retain qubit locality. The fermionic swap gate between orbitals p and q is

$$\mathcal{F}_{pq} = \exp \left[-i \frac{\pi}{2} (a_p^\dagger a_q + a_q^\dagger a_p - a_p^\dagger a_p - a_q^\dagger a_q) \right]. \quad (\text{D5})$$

This unitary is Gaussian and number-preserving, hence one may use the group homomorphism property to consolidate an arbitrarily large product of fermionic swaps into a single circuit of depth n [79, 80].

As described in Ref. [79], a total of $\lceil n/2 \rceil$ different swap circuits are required to move orbitals such that every pair is nearest-neighbor at least once. This quantity can be understood from a simple counting argument: there are $\binom{n}{2}$ off-diagonal 1-RDM elements (orbital pairs) to account for. Each ordering creates $n - 1$ nearest-neighbor pairs—therefore, we require $\binom{n}{2}/(n - 1) = n/2$ different orderings (hence unique swap circuits) to match all pairs of orbitals. In practice, this is achieved using a parallelized odd–even transposition sort.

Rounding up in the case that n is odd, and accounting for the four Pauli bases per permutation, the total number of different measurement circuits is $4\lceil n/2 \rceil + 1$.

2. The 2-RDM method

We now generalize the use of such swap networks for measuring k -RDMs. We will build up intuition with the 2-RDM. Diagonal terms are trivial as usual, since

$$a_p^\dagger a_q^\dagger a_q a_p = (1 - \delta_{pq}) \frac{I - Z_p - Z_q + Z_p Z_q}{4}. \quad (\text{D6})$$

The terms with a single occupation-number operator, restricted to 3-qubit locality, are

$$\frac{a_p^\dagger a_q^\dagger a_q a_{p+1} + \text{h.c.}}{2} = \frac{X_p X_{p+1} + Y_p Y_{p+1} - X_p X_{p+1} Z_q - Y_p Y_{p+1} Z_q}{8}, \quad (\text{D7})$$

$$\frac{a_p^\dagger a_q^\dagger a_q a_{p+1} - \text{h.c.}}{2i} = \frac{X_p Y_{p+1} - Y_p X_{p+1} - X_p Y_{p+1} Z_q + Y_p X_{p+1} Z_q}{8}, \quad (\text{D8})$$

where $q \notin \{p, p+1\}$. Lastly, we have the most general case:

$$\frac{a_p^\dagger a_{p+1}^\dagger a_q a_{q+1} + \text{h.c.}}{2} = \frac{1}{16} (-X_p X_{p+1} X_q X_{q+1} + X_p X_{p+1} Y_q Y_{q+1} - X_p Y_{p+1} X_q Y_{q+1} - X_p Y_{p+1} Y_q X_{q+1} - Y_p X_{p+1} X_q Y_{q+1} - Y_p X_{p+1} Y_q X_{q+1} + Y_p Y_{p+1} X_q X_{q+1} - Y_p Y_{p+1} Y_q Y_{q+1}), \quad (\text{D9})$$

$$\frac{a_p^\dagger a_{p+1}^\dagger a_q a_{q+1} - \text{h.c.}}{2i} = \frac{1}{16} (-X_p X_{p+1} X_q Y_{q+1} - X_p X_{p+1} Y_q X_{q+1} + X_p Y_{p+1} X_q X_{q+1} - X_p Y_{p+1} Y_q Y_{q+1} + Y_p X_{p+1} X_q X_{q+1} - Y_p X_{p+1} Y_q Y_{q+1} + Y_p Y_{p+1} X_q Y_{q+1} + Y_p Y_{p+1} Y_q X_{q+1}). \quad (\text{D10})$$

The $a_p^\dagger a_q^\dagger a_{q+1} a_{p+1}$ terms feature the same Pauli operators, but with a different sign pattern in the linear combination.

The 3- and 4-local terms are best handled separately. For the 3-local terms, the q th index is free to take any value different from p and $p+1$. We measure these qubits in the computational basis, and the p and $(p+1)$ th qubits in the same fashion as in the 1-RDM case. Then to obtain all combinations (triples) (p, p', q) , we have to swap all pairs (p, p') into, say, the qubit ordering $(0, 1)$. This allows a single ordering to account for $(n-2)$ triples. There are $\binom{n}{2}(n-2)$ total triples to permute into, and so we require $\binom{n}{2}$ different swap circuits. To measure all 8 terms, we require 4 different Pauli bases, thus $4\binom{n}{2}$ different measurement circuits. In practice we anticipate using the parallel transposition sort of the 1-RDM measurement with an additional $n-1$ measurements at each swap circuit to account for each (p, p', q) triple as $n-2$ (p, p', q) triples can be acquired simultaneously by measuring p, p' in either X or Y and all other qubits in Z .

The 4-local terms require us to swap the orbital orderings into 2-combinations of pairs in order to measure all general $a_p^\dagger a_{p'}^\dagger a_q a_{q'}$ terms. First, the number of nearest-neighbor pairs in $\{0, \dots, n-1\}$ is $n-1$. Then we count how many 2-combinations of these pairs we can construct. Note that locality between 2-combinations is not a constraint, since p and q do not have to be local. However, they must be disjoint, otherwise we are double counting the 3-local terms. Each swap circuit can account for $\binom{n-2}{2}$ different pairs of pairs; thus, since there are $\binom{n}{2} \binom{n-2}{2}$ unique $a_p^\dagger a_{p'}^\dagger a_q a_{q'}$

terms, exactly $\binom{n}{2}$ swap circuits are required. This statement is proved by a simple combinatorial argument, which we defer to the generalization in Appendix D3.

The 16 Pauli operators cannot be measured in 16 bases whenever $n > 7$. In particular, from Eq. (D9) we observe that only the $XXXX$ and $YYYY$ geminals can be measured simultaneously for $n > 7$. Therefore, in order to read off the 4-local Pauli observables, we rely on quantum overlap tomography (QOT) [31] to provide asymptotic bounds. Each (p, p', q, q') term requires measuring almost all 4-qubit marginals. More precisely, we need only the marginal elements corresponding to expectation values of Pauli operators composed of X and Y operators. QOT provides a bound for 4-qubit bound that has $\mathcal{O}(\log(n))$ scaling whenever the perfect hash family is known. Though large sets of the $(n, 4)$ -perfect hash families are documented, there remain significant gaps in n .

A more general procedure that does not achieve the same asymptotic bound of Ref. [31] is the construction of a suboptimal perfect hash family by bootstrapping from the binary partitioning scheme described in Ref. [32]. Using this approach, the leading order complexity, which upper bounds the true scaling, in the number of measurement settings is defined as the function EQOT (explicit quantum overlap tomography):

$$\text{EQOT}(k, n) = 3^k(k-1) \sum_{m=0}^{\lceil \log(n) \rceil - 1} m^{k-2}. \quad (\text{D11})$$

This gives the number of partitions to measure all k -qubit marginals, multiplied by all 3^k bases for each partition. In the case of the 4-local 2-RDM terms, however, we do not need to measure in any Pauli basis containing a Z , so we can straightforwardly reduce the base of this prefactor to 2. Altogether, we can upper bound the number of circuit configurations as

$$M_T(\text{2-RDM}) = 1 + 4 \binom{n}{2} + \binom{n}{2} \text{EQOT}(4, n) \left(\frac{2}{3}\right)^4 \quad (\text{D12})$$

circuits to measure the full fermionic 2-RDM with this approach. Again we emphasize that, though this $\text{EQOT}(4, n)$ scaling is not optimal, it will work for any n . In the following section we prove the partition scaling for the component of the k -RDM with $2k$ distinct indices, and thus the complexity, given an optimal construction of the swap circuits.

3. A k -RDM generalization

Each k -RDM observable decomposes into up to 4^k Pauli operators, thus is it impractical to write out such terms for general k by hand. Nonetheless, we can still obtain a scaling estimate on how many measurement circuits are required to reach all k -RDM elements. The following argument also applies for the 4-local terms of the 2-RDM in the previous section. Consider the asymptotically dominant terms, $a_{p_1}^\dagger \cdots a_{p_k}^\dagger a_{p_k+1} \cdots a_{p_{2k}}$ where all $p_i \neq p_j$ for $i \neq j$. There are $\binom{n}{k} \binom{n-k}{k}$ such index combinations. The number of k -combinations of disjoint nearest-neighbor pairs taken from $\{(0, 1), (1, 2), \dots, (n-2, n-1)\}$ is equivalent to counting how many unique sets of k nonconsecutive integers from $\{0, \dots, n-2\}$ exist. This is a classic “stars and bars” combinatorial problem and has solution $\binom{(n-1)-k+1}{k} = \binom{n-k}{k}$. We can see this by a visual argument: write down $(n-1) - k$ spaces where the unchosen numbers will be placed in order. Then there are $(n-1) - k - 1$ gaps in between the spaces, plus the 2 endpoints, where the chosen numbers can be placed, of which we choose k . Thus we require $\binom{n}{k}$ different swap circuits, hence $\Omega[\binom{n}{k} 4^k]$ unique measurement circuits, to reach all k -RDM elements. Similar to the 2-RDM case, this lower bound is in general not achievable, as we require (E)QOT to measure the Pauli operators in parallel, thus incurring polylogarithmic factors. We can upper bound this scaling by counting circuit repetitions for each k -RDM element partitioned by the number of unique indices.

a. Upper bounds for $k = 3, 4$

To derive an upper bound for arbitrary n in terms of measurement configurations for the 3-RDM and 4-RDM, we can follow the same procedure as the 2-RDM: count circuits for measuring RDM terms after partitioning based on the number of unique indices in each RDM element. The 3-RDM is partitioned into terms with 3, 4, 5, 6 different indices. This can be checked by building a basis for the unique 3-RDM elements indexed by a tuple (p, q, r) with $p < q < r$. The terms with only 3 unique indices are analogous to the 2-index case for the 2-RDM—e.g., the Jordan–Wigner transformation of the three index term corresponds to diagonal 3-RDM elements and thus involves only Pauli- Z

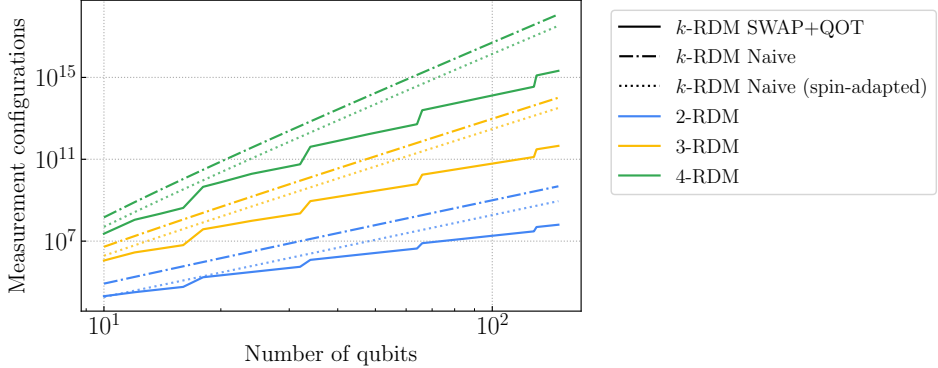


FIG. 2. Scaling of the number of measurement configurations needed while measuring the k -RDM, for $k = 2, 3, 4$ (blue, yellow, green), via the swap network protocol combined with quantum overlap tomography (solid lines) compared against the protocol where the unique upper triangle of the supermatrix representing the k -RDM is measured. For the naive measurement strategy we scale the unique number of terms in the k -RDM by 3^{2k} which is obtained by counting products of σ^+, σ^-, Z . A constant-factor improvement is possible by taking advantage of S_z -spin symmetry and only considering the spin-adapted blocks of the RDM supermatrix [13]. The swap protocol upper bound is a quadratic improvement over the naive scaling. The solid curves corresponding to the SWAP+EQOT protocol are equivalent to the orange points in Fig. 1 of the main text.

operators, as follows. All three index terms are of the form

$$a_p^\dagger a_q^\dagger a_r^\dagger a_r a_q a_p = \frac{-Z_p - Z_q - Z_r + Z_p Z_q + Z_p Z_r + Z_q Z_r - Z_p Z_q Z_r}{8} \quad (\text{D13})$$

and can be measured in one permutation of qubits (the identity permutation).

The terms with four unique indices are similar to the 3-index 2-RDM case. For example, consider the real component of a 4-index 3-RDM term,

$$a_p^\dagger a_q^\dagger a_r^\dagger a_r a_q a_{p+1} + \text{h.c.} = \frac{1}{8} [X_p X_{p+1} + Y_p Y_{p+1} + (X_p X_{p+1} + Y_p Y_{p+1})(Z_q Z_r - Z_q - Z_r)]. \quad (\text{D14})$$

These terms can be measured in $n/2$ circuits for the XX and YY parts, followed by $\binom{n}{2}$ circuits for the XXZ and YYZ terms, using the fact that $XX + YY$ commutes with ZZ , allowing us to use the measurement circuit from Ref. [54]. At each of the $n/2$ circuit configurations, all $n - 1$ pairs must account for all other Z operators. Thus in total, counting real and imaginary parts, we have a total of $4\binom{n}{2}$ qubit permutations to measure all 4-index terms.

The 5-index terms contain one Z term and can be measured with swap circuits analogous to the 4-index case in the 2-RDM. Consider the example of the real-component of the 5-index 3-RDM term,

$$a_p^\dagger a_q^\dagger a_r^\dagger a_r a_{q+1} a_{p+1} + a_{p+1}^\dagger a_{q+1}^\dagger a_r^\dagger a_r a_q a_p = \frac{1}{16} (A_{pq} + Z_r A_{pq}), \quad (\text{D15})$$

where we define

$$A_{pq} \equiv (X_p X_{p+1} X_q X_{q+1} + X_p X_{p+1} Y_q Y_{q+1} + X_p Y_{p+1} X_q Y_{q+1} - X_p Y_{p+1} Y_q X_{q+1} + Y_p X_{p+1} Y_q X_{q+1} - Y_p X_{p+1} X_q Y_{q+1} + Y_p Y_{p+1} X_q X_{q+1} + Y_p Y_{p+1} Y_q Y_{q+1}), \quad (\text{D16})$$

with $r \notin \{p, p+1, q, q+1\}$. We can obtain an upper bound for the number of unique measurements settings as $\binom{n}{k} M$, where M is the complexity of measuring 5-qubit marginals, again using the technique of Ref. [32]. The scaling for M is given in Eq. (D11) for $k = 5$ and has a prefactor of 3^5 to measure all X , Y , and Z terms. Finally, the 6-index term involves 64 separate terms, including the imaginary terms, which is measured by constructing the $\binom{n}{k}$ swap circuits and using EQOT for each permutation on the 6-qubit marginal terms which make up the 3-RDM element.

Overall, for the 3-RDM we can loosely bound the number of measurements as

$$M_T(3\text{-RDM}) = 1 + 4\binom{n}{2} + \binom{n}{2}\text{EQOT}(5) + \binom{n}{3}\text{EQOT}(6, n) \left(\frac{2}{3}\right)^6, \quad (\text{D17})$$

where each term corresponds to measuring the 3-, 4-, 5-, and 6-index terms of the 3-RDM, respectively. We note that this is an overestimate since Eq. (D11) provides an upper bound to the k -qubit marginal measurement. It is further loosened by the fact that we clearly do not need to measure *all* k -qubit marginal terms.

A similar accounting can be performed for the 4-RDM by breaking the unique 4-RDM elements into sets consisting of terms with 4, 5, 6, 7, and 8 unique indices. This gives the upper bound on measurement configurations as

$$M_T(4\text{-RDM}) = 1 + 4\binom{n}{2} + \binom{n}{2}\text{EQOT}(6, n) + \binom{n}{3}\text{EQOT}(7, n) + \binom{n}{4}\text{EQOT}(8, n) \left(\frac{2}{3}\right)^8. \quad (\text{D18})$$

In Fig. 2 we plot the scaling of the swap network EQOT protocol against naively measuring the upper triangle of unique k -RDM elements in a supermatrix representation, as a function of the number of fermionic modes.

Appendix E: Supplementary numerical calculations

Here we provide some additional findings with our numerical studies. These are not essential to the primary results of the main text, but rather serve to explore some of the more subtler points of our partial tomography scheme.

1. Hyperparameter tuning

As mentioned in the main text, we may control how many circuits to randomly generate by setting a hyperparameter r such that all K_r unitaries correspond to measurements of all observables at least r times each. Since increasing the sample size decreases the frequency of outlier events (e.g., that some subset of observables being accounted for more often than the rest), we then expect that the value of K_r/r should in fact decrease as a function of r . Indeed, this is a generic feature of randomization, as observed in the numerical results of the original work on classical shadows [38]. This effect is demonstrated, with the 2-RDM as an example, in Fig. 3. The behavior is consistent as expected.

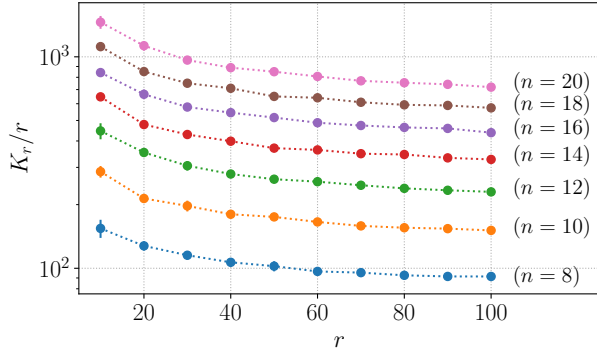


FIG. 3. The relation between K_r/r and r for various numbers of modes under the \mathcal{U}_{FGU} ensemble, with respect to covering 2-RDM observables. Since K_r is a random variable, we average over 10 randomly generated circuit collections for each r and indicate 1 standard deviation with uncertainty bars.

2. Realistic time estimates

The main experimental difference between deterministic and randomized measurement schemes is the number of unique circuits one must run. In general, the number of random unitaries (K_r) will be larger than the deterministic clique cover size (C). Thus depending on the architecture, reprogramming the quantum device for each new circuit may incur a nontrivial overhead in the actual wall-clock time of the algorithm. Here, we show that for realistic experimental parameters, this consideration does not affect the results presented in the main text.

Suppose the quantum device can repeatedly sample a fixed circuit at a rate f_{samp} , but requires time t_{load} to load a new circuit. Then the total measurement time under the two paradigms are

$$T_{\text{deter}} = C \left(\frac{S}{f_{\text{samp}}} + t_{\text{load}} \right), \quad (\text{E1})$$

$$T_{\text{rand}} = K_r \left(\frac{\lceil S/r \rceil}{f_{\text{samp}}} + t_{\text{load}} \right), \quad (\text{E2})$$

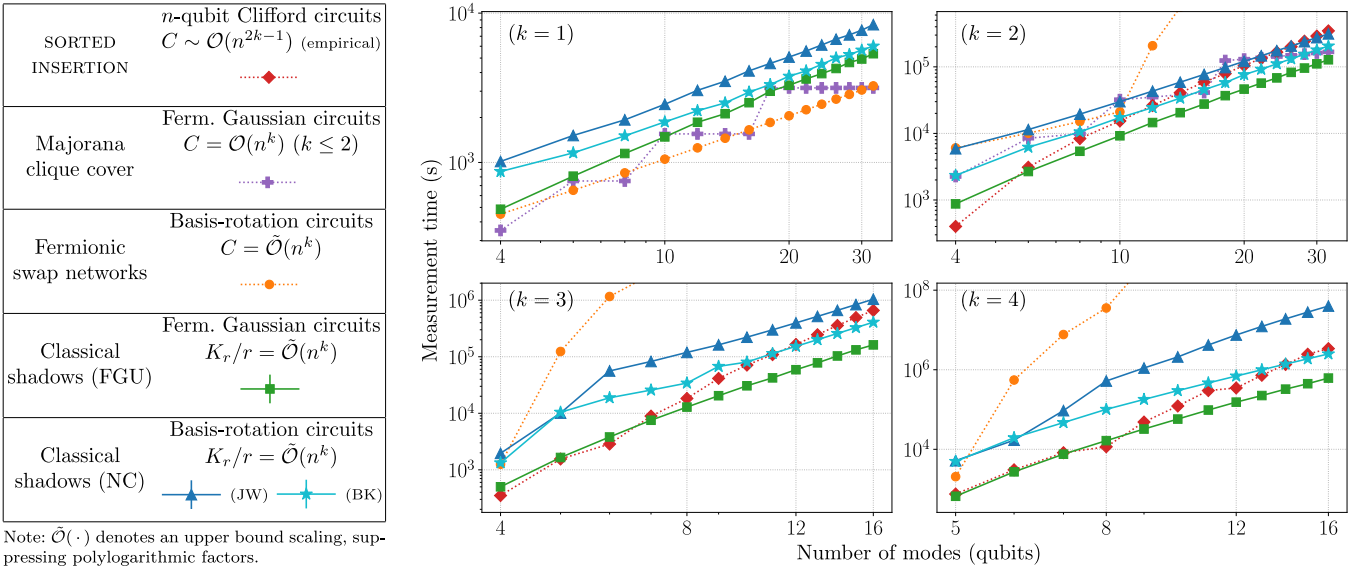


FIG. 4. Measurement times for estimating k -RDMs, calculated with Eqs. (E1) and (E2), under the reported device parameters of the Google Sycamore chip [98] and with $S = 2.5 \times 10^5$. The underlying data is that of Fig. 1 in the main text. For convenience, we reproduce the table/legend of the main text here as well.

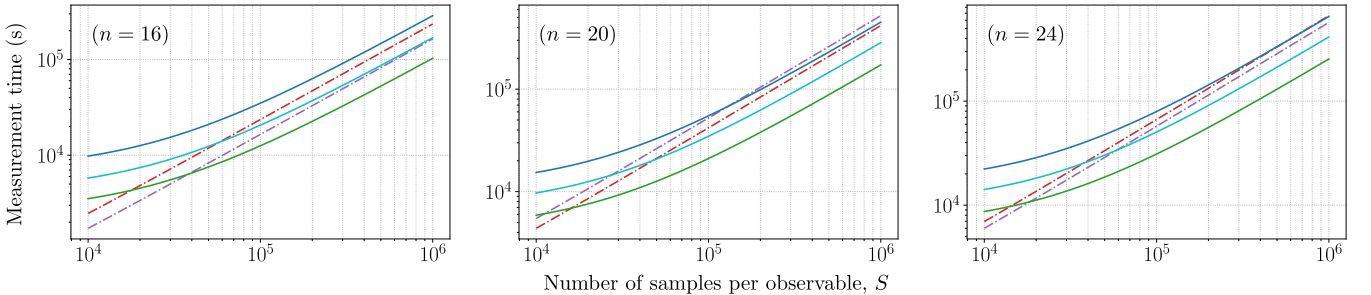


FIG. 5. Examples of how the measurement times for our randomized schemes scale with the accuracy level, as given by Eq. (E2). We use the same device parameters here as in Fig. 4. For comparison, we also plot the linear scaling of the prior deterministic strategies (excluding the swap network method), which gives us an indication for which values of S we obtain an advantage with our methods under this time-cost model. The colors correspond to those in the legend of Fig. 4.

where we recall that $S = \mathcal{O}(1/\varepsilon^2)$. Note that in the regime where $S \gg f_{\text{samp}} t_{\text{load}}$, we may directly compare C to K_r/r , as in the main text. For hardware-dependent estimates, we take the specifications of the Google Sycamore chip as an example [54, 95–97]. The reported parameter values are $f_{\text{samp}} = 5 \times 10^3$ Hz and $t_{\text{load}} = 0.1$ s [98], and for Fig. 4, we set $S = 2.5 \times 10^5$, in line with the number of shots taken to estimate 1-RDM elements in a recent Hartree–Fock experiment [54]. We observe no qualitative differences from the results of the main text.

One may also study the performance of the different methods as a function of the target accuracy. In Fig. 5, we show how T_{rand} scales with S for the 2-RDM, using a few values of n as illustrative examples. Though the threshold at which randomization begins to outperform the other methods varies depending on n and k , it typically lies below $\sim 10^5$, which is well under practical accuracy levels. Note that the $S \gg f_{\text{samp}} t_{\text{load}}$ regime corresponds to when T_{rand} scales linearly with S .

3. Hamiltonian averaging

In the context of estimating a single observable, whose expectation value is a linear combination of RDM elements, the number of circuit repetitions required is more properly determined by taking into account the coefficients of the terms and covariances between simultaneously measured terms [8, 9, 13]. This can be directly calculated from the (single-shot) variance of the corresponding estimator. Here we provide some preliminary numerical calculations in

this context, with respect to \mathcal{U}_{FGU} . Although our uniformly distributed ensemble is not tailored for Hamiltonian averaging, these calculations provide a benchmark for improvement.

Without loss of generality, consider a traceless fermionic Hamiltonian

$$H = \sum_{k=1}^n \sum_{\mu \in \mathcal{C}_{2n,2k}} h_{\mu} \Gamma_{\mu}, \quad h_{\mu} \in \mathbb{R}. \quad (\text{E3})$$

From the results of Appendix B 4, we can calculate the variance of its classical shadows estimator as

$$\text{Var}_{Q,z}[\text{tr}(H \hat{\rho}_{Q,z})] = \sum_{k=1}^n \sum_{\mu \in \mathcal{C}_{2n,2k}} \|h_{\mu} \Gamma_{\mu}\|_{\text{FGU}}^2 - \text{tr}(H \rho)^2. \quad (\text{E4})$$

While this expression holds for an arbitrary even-degree observable, the weights h_{μ} of physical Hamiltonians are usually nonzero only up to $k = 2$ (e.g., in electronic structure). In particular, we numerically studied a sample of molecular Hamiltonians at equilibrium nuclear geometry, obtained through OpenFermion [83] interfaced with the Psi4 electronic structure package [99]. We used a minimal STO-3G orbital basis set to calculate these Hamiltonians, except for the H_2 molecule, which was represented in the 6-31G basis.

In Table I we compare our classical shadows (CS) \mathcal{U}_{FGU} ensemble against two prominent methods for electronic structure: a strategy based on a low-rank factorization of the coefficient tensor, termed basis-rotation grouping (BRG) [16], and a locally biased adaptation on classical shadows (LBCS) [23]. For reference, we also report the variance under standard classical shadows with Pauli measurements [38]. Note that, in order to compare fairly between the deterministic (BRG) and randomized methods (CS, LBCS), we reframe the deterministic measurement scheduling such that an equivalent variance quantity may be computed. This principle was also used in the numerical comparisons of Ref. [23], which we generalize below.

We decompose the target Hamiltonian as

$$H = \sum_{\ell=1}^L O_{\ell}, \quad (\text{E5})$$

where each $\text{tr}(O_{\ell} \rho)$ may be estimated by a single measurement setting (as defined by the given strategy). The optimal distribution of measurements then allocates a fraction

$$p_{\ell} := \frac{\sqrt{\text{Var}_{\rho}[O_{\ell}]}}{\sum_{j=1}^L \sqrt{\text{Var}_{\rho}[O_j]}} \quad (\text{E6})$$

of the total measurement budget to the ℓ th setting [13]. The variance here is simply the quantum-mechanical operator variance,

$$\text{Var}_{\rho}[O_{\ell}] = \text{tr}(O_{\ell}^2 \rho) - \text{tr}(O_{\ell} \rho)^2. \quad (\text{E7})$$

Recognizing $\{p_{\ell}\}_{\ell}$ as a collection of positive numbers which sum to unity, we may recast the deterministic strategy into the language of randomization, where the unbiased estimator is given by

$$\mathbb{E}_{\ell,\rho} \left[\frac{1}{p_{\ell}} O_{\ell} \right] = \mathbb{E}_{\ell} \left[\frac{1}{p_{\ell}} \text{tr}(O_{\ell} \rho) \right] = \text{tr}(H \rho). \quad (\text{E8})$$

The variance of this estimator is therefore

$$\begin{aligned} \text{Var}_{\ell,\rho} \left[\frac{1}{p_{\ell}} O_{\ell} \right] &= \mathbb{E}_{\ell,\rho} \left[\frac{1}{p_{\ell}^2} O_{\ell}^2 \right] - \mathbb{E}_{\ell,\rho} \left[\frac{1}{p_{\ell}} O_{\ell} \right]^2 \\ &= \sum_{\ell=1}^L \frac{1}{p_{\ell}} \text{tr}(O_{\ell}^2 \rho) - \text{tr}(H \rho)^2. \end{aligned} \quad (\text{E9})$$

Note that this analysis does not actually require a randomization the deterministic strategy, but merely normalizes the measurement allocations so as to produce an equivalent figure of merit.

While Eq. (E6) provides the optimal distribution of measurements, one may use any distribution in its place. In particular, because ρ is unknown, a state-independent approximation to $\{p_{\ell}\}_{\ell}$ is often a more practical option; tighter

TABLE I. Variances of Hamiltonian averaging estimators under various strategies, reported in units of Ha^2 . The expressions for the CS (Pauli) and LBCS variances may be found in their original references, although the fundamental formula for all table entries is given by Eq. (E9), where the decomposition into measurable terms O_ℓ and probabilities p_ℓ are determined by the particular method. The reference state used here is an exact ground state calculation.

| Molecule (qubits) | Methods | | | | |
|---------------------------|-----------------|-----------|----------|----------|--|
| | CS (Pauli) [38] | LBCS [23] | BRG [16] | CS (FGU) | |
| H_2 (8) | 51.4 | 17.5 | 22.6 | 74.7 | |
| LiH (12) | 266 | 14.8 | 7.0 | 146 | |
| BeH_2 (14) | 1670 | 67.6 | 68.3 | 554 | |
| H_2O (14) | 2840 | 257 | 6559 | 9042 | |
| NH_3 (16) | 14400 | 353 | 3288 | 6147 | |

bounds may be obtained by a classically tractable approximation to the true, unknown state. For simplicity, in Table I we take ρ as the exact ground state within the model chemistry. We note that Ref. [16] showed evidence that the discrepancy between using the exact ground state and the state obtained from a configuration interaction with single and double excitations (CISD) calculation is negligible in this context.

Our main takeaway from Table I is that, similar to how Pauli measurements can be dramatically improved via solving an optimization problem targeted specifically at minimizing this variance [23], our classical shadows method similarly has a large room for improvement. Since only LBCS performs such an optimization, it is perhaps not too surprising that it is the most efficient approach here, despite only employing Pauli measurements. Encouragingly, such a biasing (or similar optimization-based extensions) may also be applied to our classical shadows ensemble in principle. It should be noted that these results assume the noiseless case; for instance, the BRG strategy additionally offers resilience to device errors and the ability to postselect on particle number, which have the effect of reducing noise-induced contributions to the variance [16].

[1] M. A. Nielsen and I. Chuang, *Quantum Computation and Quantum Information* (Cambridge University Press, 2010).
[2] A. Y. Kitaev, A. Shen, and M. N. Vyalyi, *Classical and Quantum Computation* (American Mathematical Society, 2002).
[3] D. S. Abrams and S. Lloyd, Quantum algorithm providing exponential speed increase for finding eigenvalues and eigenvectors, *Physical Review Letters* **83**, 5162 (1999).
[4] R. Somma, G. Ortiz, J. E. Gubernatis, E. Knill, and R. Laflamme, Simulating physical phenomena by quantum networks, *Physical Review A* **65**, 042323 (2002).
[5] A. Aspuru-Guzik, A. D. Dutoi, P. J. Love, and M. Head-Gordon, Simulated quantum computation of molecular energies, *Science* **309**, 1704 (2005).
[6] J. Preskill, Quantum computing in the NISQ era and beyond, *Quantum* **2**, 79 (2018).
[7] A. Peruzzo, J. McClean, P. Shadbolt, M.-H. Yung, X.-Q. Zhou, P. J. Love, A. Aspuru-Guzik, and J. L. O’Brien, A variational eigenvalue solver on a photonic quantum processor, *Nature Communications* **5**, 4213 (2014).
[8] J. R. McClean, J. Romero, R. Babbush, and A. Aspuru-Guzik, The theory of variational hybrid quantum-classical algorithms, *New Journal of Physics* **18**, 023023 (2016).
[9] D. Wecker, M. B. Hastings, and M. Troyer, Progress towards practical quantum variational algorithms, *Physical Review A* **92**, 042303 (2015).
[10] J. R. McClean, R. Babbush, P. J. Love, and A. Aspuru-Guzik, Exploiting locality in quantum computation for quantum chemistry, *The Journal of Physical Chemistry Letters* **5**, 4368 (2014).
[11] A. Kandala, A. Mezzacapo, K. Temme, M. Takita, M. Brink, J. M. Chow, and J. M. Gambetta, Hardware-efficient variational quantum eigensolver for small molecules and quantum magnets, *Nature* **549**, 242 (2017).
[12] R. Babbush, N. Wiebe, J. McClean, J. McClain, H. Neven, and G. K.-L. Chan, Low-depth quantum simulation of materials, *Physical Review X* **8**, 011044 (2018).
[13] N. C. Rubin, R. Babbush, and J. McClean, Application of fermionic marginal constraints to hybrid quantum algorithms, *New Journal of Physics* **20**, 053020 (2018).
[14] A. F. Izmaylov, T.-C. Yen, and I. G. Ryabinkin, Revising the measurement process in the variational quantum eigensolver: is it possible to reduce the number of separately measured operators?, *Chemical Science* **10**, 3746 (2019).
[15] A. F. Izmaylov, T.-C. Yen, R. A. Lang, and V. Verteletskyi, Unitary partitioning approach to the measurement problem in the variational quantum eigensolver method, *Journal of Chemical Theory and Computation* **16**, 190 (2019).
[16] W. J. Huggins, J. McClean, N. Rubin, Z. Jiang, N. Wiebe, K. B. Whaley, and R. Babbush, Efficient and noise resilient measurements for quantum chemistry on near-term quantum computers, [arXiv:1907.13117](https://arxiv.org/abs/1907.13117) (2019).
[17] O. Crawford, B. van Straaten, D. Wang, T. Parks, E. Campbell, and S. Brierley, Efficient quantum measurement of Pauli operators, [arXiv:1908.06942](https://arxiv.org/abs/1908.06942) (2019).

- [18] A. Zhao, A. Tranter, W. M. Kirby, S. F. Ung, A. Miyake, and P. J. Love, Measurement reduction in variational quantum algorithms, *Physical Review A* **101**, 062322 (2020).
- [19] G. Torlai, G. Mazzola, G. Carleo, and A. Mezzacapo, Precise measurement of quantum observables with neural-network estimators, *Physical Review Research* **2**, 022060 (2020).
- [20] A. Arrasmith, L. Cincio, R. D. Somma, and P. J. Coles, Operator sampling for shot-frugal optimization in variational algorithms, [arXiv:2004.06252](https://arxiv.org/abs/2004.06252) (2020).
- [21] G. Wang, D. E. Koh, P. D. Johnson, and Y. Cao, Bayesian inference with engineered likelihood functions for robust amplitude estimation, [arXiv:2006.09350](https://arxiv.org/abs/2006.09350) (2020).
- [22] M. Paini and A. Kalev, An approximate description of quantum states, [arXiv:1910.10543](https://arxiv.org/abs/1910.10543) (2019).
- [23] C. Hadfield, S. Bravyi, R. Raymond, and A. Mezzacapo, Measurements of quantum Hamiltonians with locally-biased classical shadows, [arXiv:2006.15788](https://arxiv.org/abs/2006.15788) (2020).
- [24] T.-C. Yen and A. F. Izmaylov, Cartan sub-algebra approach to efficient measurements of quantum observables, [arXiv:2007.01234](https://arxiv.org/abs/2007.01234) (2020).
- [25] S. Aaronson, Shadow tomography of quantum states, *SIAM Journal on Computing* , 368 (2020); S. Aaronson, X. Chen, E. Hazan, S. Kale, and A. Nayak, Online learning of quantum states, in *Advances in Neural Information Processing Systems* (2018) pp. 8962–8972; S. Aaronson and G. N. Rothblum, Gentle measurement of quantum states and differential privacy, in *Proceedings of the 51st Annual ACM SIGACT Symposium on Theory of Computing* (2019) pp. 322–333.
- [26] N. Yu, Quantum closeness testing: a streaming algorithm and applications, [arXiv:1904.03218](https://arxiv.org/abs/1904.03218) (2019); Sample efficient tomography via Pauli measurements, [arXiv:2009.04610](https://arxiv.org/abs/2009.04610) (2020).
- [27] V. Verteletskyi, T.-C. Yen, and A. F. Izmaylov, Measurement optimization in the variational quantum eigensolver using a minimum clique cover, *The Journal of Chemical Physics* **152**, 124114 (2020).
- [28] A. Jena, S. Genin, and M. Mosca, Pauli partitioning with respect to gate sets, [arXiv:1907.07859](https://arxiv.org/abs/1907.07859) (2019).
- [29] T.-C. Yen, V. Verteletskyi, and A. F. Izmaylov, Measuring all compatible operators in one series of single-qubit measurements using unitary transformations, *Journal of Chemical Theory and Computation* **16**, 2400 (2020).
- [30] P. Gokhale, O. Angiuli, Y. Ding, K. Gui, T. Tomesh, M. Suchara, M. Martonosi, and F. T. Chong, Minimizing state preparations in variational quantum eigensolver by partitioning into commuting families, [arXiv:1907.13623](https://arxiv.org/abs/1907.13623) (2019).
- [31] J. Cotler and F. Wilczek, Quantum overlapping tomography, *Physical Review Letters* **124**, 100401 (2020).
- [32] X. Bonet-Monroig, R. Babbush, and T. E. O’Brien, Nearly optimal measurement scheduling for partial tomography of quantum states, *Physical Review X* **10**, 031064 (2020).
- [33] P. Gokhale and F. T. Chong, $O(N^3)$ measurement cost for variational quantum eigensolver on molecular Hamiltonians, [arXiv:1908.11857](https://arxiv.org/abs/1908.11857) (2019).
- [34] I. Hamamura and T. Imamichi, Efficient evaluation of quantum observables using entangled measurements, *npj Quantum Information* **6**, 1 (2020).
- [35] G. García-Pérez, M. A. Rossi, B. Sokolov, E.-M. Borrelli, and S. Maniscalco, Pairwise tomography networks for many-body quantum systems, *Physical Review Research* **2**, 023393 (2020).
- [36] Z. Jiang, A. Kalev, W. Mruczkiewicz, and H. Neven, Optimal fermion-to-qubit mapping via ternary trees with applications to reduced quantum states learning, *Quantum* **4**, 276 (2020).
- [37] T. J. Evans, R. Harper, and S. T. Flammia, Scalable Bayesian Hamiltonian learning, [arXiv:1912.07636](https://arxiv.org/abs/1912.07636) (2019).
- [38] H.-Y. Huang, R. Kueng, and J. Preskill, Predicting many properties of a quantum system from very few measurements, *Nature Physics* **16**, 1050 (2020).
- [39] A. Harrow and J. Napp, Low-depth gradient measurements can improve convergence in variational hybrid quantum-classical algorithms, [arXiv:1901.05374](https://arxiv.org/abs/1901.05374) (2019).
- [40] D. Wang, O. Higgott, and S. Brierley, Accelerated variational quantum eigensolver, *Physical Review Letters* **122**, 140504 (2019).
- [41] J. M. Kübler, A. Arrasmith, L. Cincio, and P. J. Coles, An adaptive optimizer for measurement-frugal variational algorithms, *Quantum* **4**, 263 (2020).
- [42] R. Sweke, F. Wilde, J. J. Meyer, M. Schuld, P. K. Fährmann, B. Meynard-Piganeau, and J. Eisert, Stochastic gradient descent for hybrid quantum-classical optimization, *Quantum* **4**, 314 (2020).
- [43] B. van Straaten and B. Koczor, Measurement cost of metric-aware variational quantum algorithms, [arXiv:2005.05172](https://arxiv.org/abs/2005.05172) (2020).
- [44] A. Coleman and I. Absar, Reduced Hamiltonian orbitals. III. Unitarily invariant decomposition of Hermitian operators, *International Journal of Quantum Chemistry* **18**, 1279 (1980).
- [45] S. Tsuneyuki, Transcorrelated method: another possible way towards electronic structure calculation of solids, *Progress of Theoretical Physics Supplement* **176**, 134 (2008).
- [46] M. R. Peterson and C. Nayak, More realistic Hamiltonians for the fractional quantum Hall regime in GaAs and graphene, *Physical Review B* **87**, 245129 (2013).
- [47] D. A. Mazziotti, Two-electron reduced density matrix as the basic variable in many-electron quantum chemistry and physics, *Chemical Reviews* **112**, 244 (2012).
- [48] F. Jensen, *Introduction to Computational Chemistry* (John Wiley & Sons, 2017).
- [49] J. R. McClean, M. E. Kimchi-Schwartz, J. Carter, and W. A. De Jong, Hybrid quantum-classical hierarchy for mitigation of decoherence and determination of excited states, *Physical Review A* **95**, 042308 (2017).
- [50] T. Takeshita, N. C. Rubin, Z. Jiang, E. Lee, R. Babbush, and J. R. McClean, Increasing the representation accuracy of quantum simulations of chemistry without extra quantum resources, *Physical Review X* **10**, 011004 (2020).
- [51] J. I. Colless, V. V. Ramasesh, D. Dahlen, M. S. Blok, M. Kimchi-Schwartz, J. McClean, J. Carter, W. De Jong, and

I. Siddiqi, Computation of molecular spectra on a quantum processor with an error-resilient algorithm, *Physical Review X* **8**, 011021 (2018).

[52] R. Sagastizabal, X. Bonet-Monroig, M. Singh, M. A. Rol, C. Bultink, X. Fu, C. Price, V. Ostroukh, N. Muthusubramanian, A. Bruno, *et al.*, Experimental error mitigation via symmetry verification in a variational quantum eigensolver, *Physical Review A* **100**, 010302 (2019).

[53] A. J. McCaskey, Z. P. Parks, J. Jakowski, S. V. Moore, T. D. Morris, T. S. Humble, and R. C. Pooser, Quantum chemistry as a benchmark for near-term quantum computers, *npj Quantum Information* **5**, 1 (2019).

[54] Google AI Quantum and Collaborators, Hartree-Fock on a superconducting qubit quantum computer, *Science* **369**, 1084 (2020).

[55] H. R. Grimsley, S. E. Economou, E. Barnes, and N. J. Mayhall, An adaptive variational algorithm for exact molecular simulations on a quantum computer, *Nature Communications* **10**, 1 (2019).

[56] I. G. Ryabinkin, R. A. Lang, S. N. Genin, and A. F. Izmaylov, Iterative qubit coupled cluster approach with efficient screening of generators, *Journal of Chemical Theory and Computation* **16**, 1055 (2020).

[57] H. L. Tang, E. Barnes, H. R. Grimsley, N. J. Mayhall, and S. E. Economou, qubit-ADAPT-VQE: An adaptive algorithm for constructing hardware-efficient ansatze on a quantum processor, *arXiv:1911.10205* (2019).

[58] Q. Wang, M. Li, C. Monroe, and Y. Nam, Resource-optimized fermionic local-hamiltonian simulation on quantum computer for quantum chemistry, *arXiv:2004.04151* (2020).

[59] R. M. Parrish, E. G. Hohenstein, P. L. McMahon, and T. J. Martínez, Quantum computation of electronic transitions using a variational quantum eigensolver, *Physical Review Letters* **122**, 230401 (2019).

[60] W. J. Huggins, J. Lee, U. Baek, B. O'Gorman, and K. B. Whaley, A non-orthogonal variational quantum eigensolver, *New Journal of Physics* **22**, 073009 (2020).

[61] N. H. Stair, R. Huang, and F. A. Evangelista, A multireference quantum Krylov algorithm for strongly correlated electrons, *Journal of Chemical Theory and Computation* **16**, 2236 (2020).

[62] M. Urbanek, D. Camps, R. Van Beeumen, and W. A. de Jong, Chemistry on quantum computers with virtual quantum subspace expansion, *Journal of Chemical Theory and Computation* **16**, 5425 (2020).

[63] P. Jordan and E. Wigner, Über das Paulische Äquivalenzverbot, *Z. Phys.* **47**, 631 (1928).

[64] S. B. Bravyi and A. Y. Kitaev, Fermionic quantum computation, *Annals of Physics* **298**, 210 (2002).

[65] J. T. Seeley, M. J. Richard, and P. J. Love, The Bravyi–Kitaev transformation for quantum computation of electronic structure, *The Journal of Chemical Physics* **137**, 224109 (2012).

[66] A. Tranter, S. Sofia, J. Seeley, M. Kaicher, J. McClean, R. Babbush, P. V. Coveney, F. Mintert, F. Wilhelm, and P. J. Love, The Bravyi–Kitaev transformation: Properties and applications, *International Journal of Quantum Chemistry* **115**, 1431 (2015).

[67] V. Havlíček, M. Troyer, and J. D. Whitfield, Operator locality in the quantum simulation of fermionic models, *Physical Review A* **95**, 032332 (2017).

[68] D. Sattinger and O. Weaver, *Lie Groups and Algebras with Applications to Physics, Geometry, and Mechanics* (Springer-Verlag New York, 1986).

[69] E. Knill, Fermionic linear optics and matchgates, *arXiv:quant-ph/0108033* (2001).

[70] B. M. Terhal and D. P. DiVincenzo, Classical simulation of noninteracting-fermion quantum circuits, *Physical Review A* **65**, 032325 (2002).

[71] S. Bravyi, Lagrangian representation for fermionic linear optics, *Quantum Information and Computation* **5**, 216 (2005).

[72] D. P. DiVincenzo and B. M. Terhal, Fermionic linear optics revisited, *Foundations of Physics* **35**, 1967 (2005).

[73] R. Jozsa and A. Miyake, Matchgates and classical simulation of quantum circuits, *Proceedings of the Royal Society A: Mathematical, Physical and Engineering Sciences* **464**, 3089 (2008).

[74] D. Gottesman, The Heisenberg representation of quantum computers, *arXiv:quant-ph/9807006* (1998).

[75] S. Aaronson and D. Gottesman, Improved simulation of stabilizer circuits, *Physical Review A* **70**, 052328 (2004).

[76] A. Chapman and A. Miyake, Classical simulation of quantum circuits by dynamical localization: Analytic results for Pauli-observable scrambling in time-dependent disorder, *Physical Review A* **98**, 012309 (2018).

[77] W. Hoeffding, Probability inequalities for sums of bounded random variables, *Journal of the American Statistical Association* **58**, 13 (1963).

[78] D. Wecker, M. B. Hastings, N. Wiebe, B. K. Clark, C. Nayak, and M. Troyer, Solving strongly correlated electron models on a quantum computer, *Physical Review A* **92**, 062318 (2015).

[79] I. D. Kivlichan, J. McClean, N. Wiebe, C. Gidney, A. Aspuru-Guzik, G. K.-L. Chan, and R. Babbush, Quantum simulation of electronic structure with linear depth and connectivity, *Physical Review Letters* **120**, 110501 (2018).

[80] Z. Jiang, K. J. Sung, K. Kechedzhi, V. N. Smelyanskiy, and S. Boixo, Quantum algorithms to simulate many-body physics of correlated fermions, *Physical Review Applied* **9**, 044036 (2018).

[81] X. Bonet-Monroig, R. Sagastizabal, M. Singh, and T. E. O'Brien, Low-cost error mitigation by symmetry verification, *Physical Review A* **98**, 062339 (2018).

[82] S. McArdle, X. Yuan, and S. Benjamin, Error-mitigated digital quantum simulation, *Physical Review Letters* **122**, 180501 (2019).

[83] J. R. McClean, N. C. Rubin, K. J. Sung, I. D. Kivlichan, X. Bonet-Monroig, Y. Cao, C. Dai, E. S. Fried, C. Gidney, B. Gimby, *et al.*, OpenFermon: the electronic structure package for quantum computers, *Quantum Science and Technology* **5**, 034014 (2020).

[84] P. Raghavan, Probabilistic construction of deterministic algorithms: approximating packing integer programs, *Journal of Computer and System Sciences* **37**, 130 (1988).

- [85] N. Alon and J. H. Spencer, *The Probabilistic Method* (John Wiley & Sons, 2004).
- [86] R. F. Streater and A. S. Wightman, *PCT, Spin and Statistics, and All That* (Princeton University Press, 2000).
- [87] M. Steudtner and S. Wehner, Fermion-to-qubit mappings with varying resource requirements for quantum simulation, *New Journal of Physics* **20**, 063010 (2018).
- [88] J. Lawrence, Č. Brukner, and A. Zeilinger, Mutually unbiased binary observable sets on N qubits, *Physical Review A* **65**, 032320 (2002).
- [89] D. Han and D. R. Larson, *Frames, Bases and Group Representations* (American Mathematical Society, 2000).
- [90] S. F. Waldron, *An Introduction to Finite Tight Frames* (Birkhäuser Basel, 2018).
- [91] R. Vale and S. Waldron, Tight frames and their symmetries, *Constructive Approximation* **21**, 83 (2004).
- [92] N. Cotfas and J. P. Gazeau, Finite tight frames and some applications, *Journal of Physics A: Mathematical and Theoretical* **43**, 193001 (2010).
- [93] P. A. Grillet, *Abstract Algebra* (Springer-Verlag New York, 2007).
- [94] W. Fulton and J. Harris, *Representation Theory: A First Course* (Springer-Verlag New York, 2004).
- [95] F. Arute, K. Arya, R. Babbush, D. Bacon, J. C. Bardin, R. Barends, R. Biswas, S. Boixo, F. G. S. L. Brandao, D. A. Buell, *et al.*, Quantum supremacy using a programmable superconducting processor, *Nature* **574**, 505 (2019).
- [96] Google AI Quantum and Collaborators, Quantum approximate optimization of non-planar graph problems on a planar superconducting processor, [arXiv:2004.04197](https://arxiv.org/abs/2004.04197) (2020).
- [97] Google AI Quantum and Collaborators, Observation of separated dynamics of charge and spin in the Fermi-Hubbard model, [arXiv:2010.07965](https://arxiv.org/abs/2010.07965) (2020).
- [98] K. J. Sung, M. P. Harrigan, N. C. Rubin, Z. Jiang, R. Babbush, and J. R. McClean, An exploration of practical optimizers for variational quantum algorithms on superconducting qubit processors, [arXiv:2005.11011](https://arxiv.org/abs/2005.11011) (2020).
- [99] R. M. Parrish, L. A. Burns, D. G. Smith, A. C. Simmonett, A. E. DePrince III, E. G. Hohenstein, U. Bozkaya, A. Y. Sokolov, R. Di Remigio, R. M. Richard, *et al.*, Psi4 1.1: An open-source electronic structure program emphasizing automation, advanced libraries, and interoperability, *Journal of Chemical Theory and Computation* **13**, 3185 (2017).